Optical Imaging Based on Photo-Acoustic Techniques

台大電機系李百祺

There is more than light,…

Opto-acoustic (Photo-acoustic) imaging:

Imaging with optically generated ultrasound

Essentials of Imaging

- Contrast mechanism
- Spatial resolution
- Sensitivity
- Wave generation and detection
- Image formation
- Sources of distortion
- Limitations

Motivations for OA Imaging

- Thermoelastic effects.
- Contrast mechanism is based on optical differences. Major chromophores in VIS-NIR are hemoglobin and melanin.
- Acoustic propagation is used for reducing distortion effects.
- Combining advantages of optical and ultrasonic imaging.

Basic Principles of OA Imaging

- Light absorption
- Irradiation and detection.
- Forward and backward modes
- Signal processing for compensating signal distortion.

Applications of OA Imaging

- Breast imaging
  - Deep lying structures
  - Requiring good sensitivity
- Skin profiling
  - Detection and staging of cancer
  - Requiring good resolution
- Functional and molecular imaging
- Many more,…

Time-Resolved Opto-Acoustic Detection

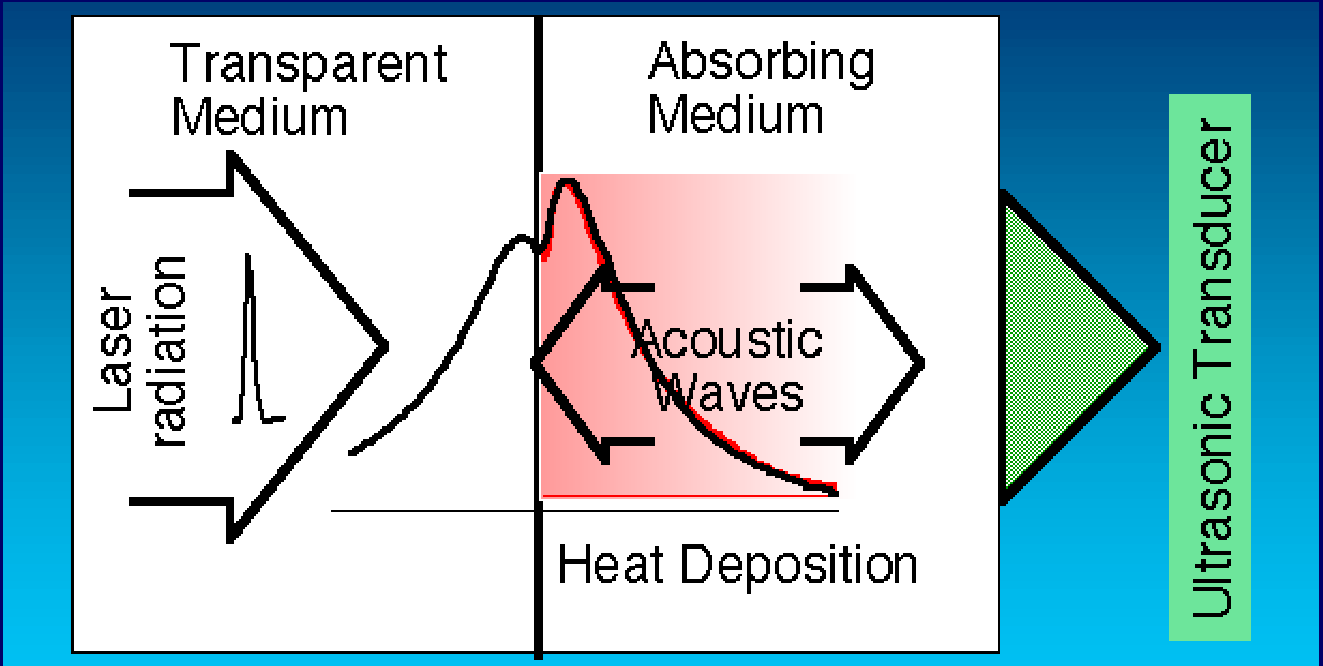

$\tau_L < 1/\mu_a C_s$ laser-induced pressure must be confined in the volume of diagnostic interest

Absorbed Energy Distribution

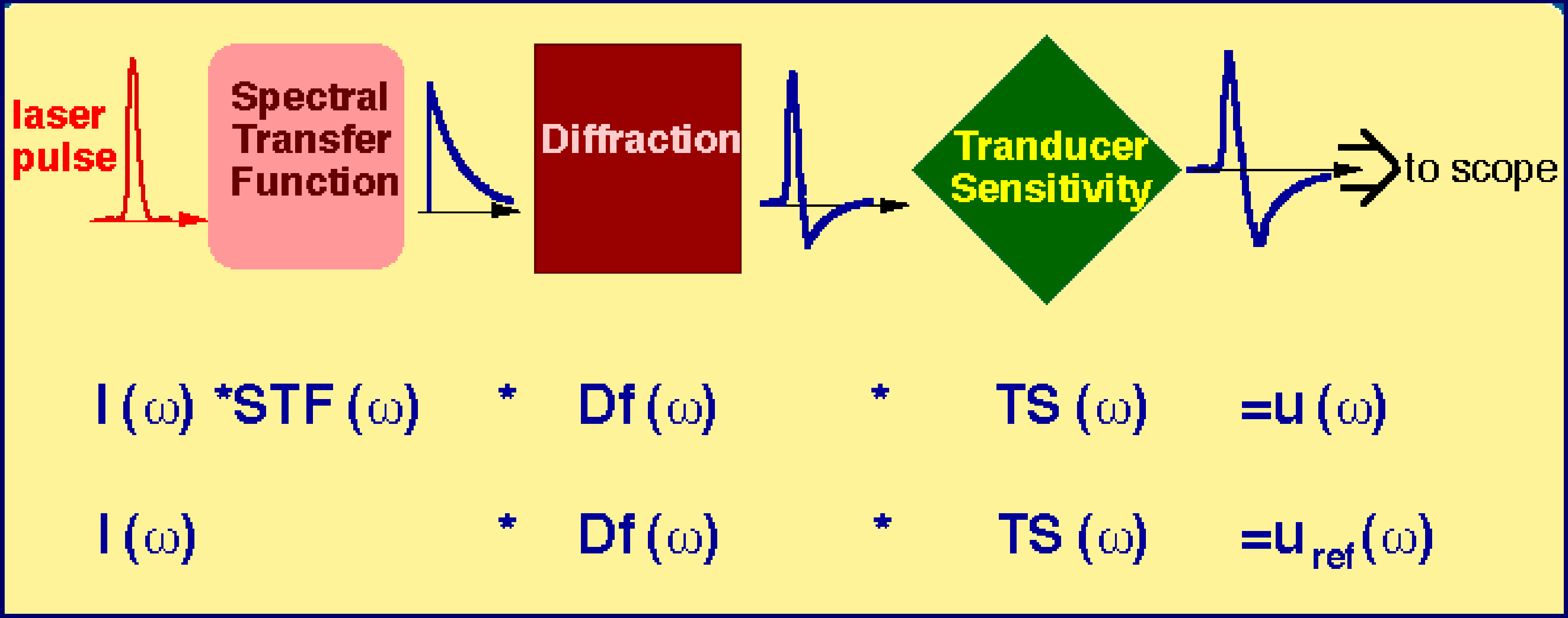

Laser-Induced Acoustic Waveform: Small Absorbing Sphere

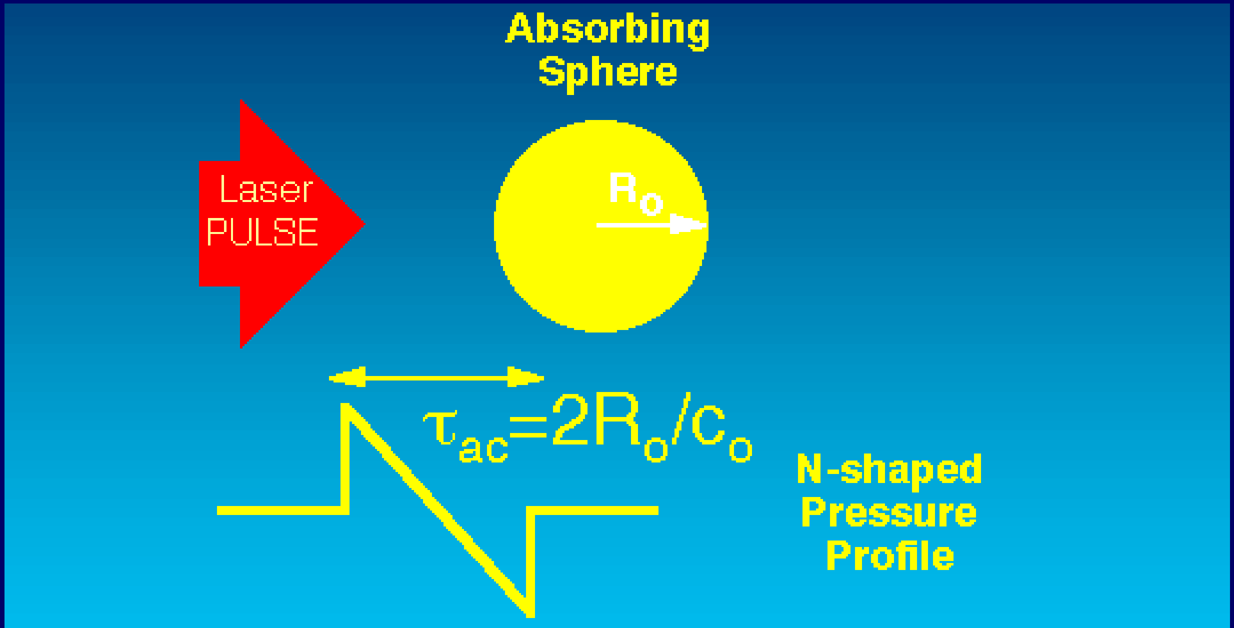

$$p(\tau = t - r/c_0) = \frac{1}{4\pi r}\frac{\beta c_0^2}{c_p}\frac{3E_{abs}}{2R_0^3}\begin{cases} -c_0\tau, & |c_0\tau| \le R_o; \\ 0, & |c_0\tau| \ge R_o; \end{cases}$$

Sensitivity and Resolution

- Opto-acoustic signals are wide-band, ultrasonic transients.
- Sensitivity is spread over the bandwidth.
- Main parameter of transducer in OA imaging: $\Delta S/\Delta f_{ac}$ (bandwidth specific sensitivity).
- Typical transducer materials: PZT, PVDF and Lithium Niobate.

Outline

- Basics in acoustics:
  - Wave propagation
  - Scattering, attenuation and speckle
  - Fundamental limitation in image contrast
- Acoustic generation and detection
- Optical detection of ultrasonic displacement
- Optical generation by laser
- Applications:
  - OA imaging
  - Ultrasonic imaging

Acoustic Wave Propagation

Basics of Acoustic Waves

- A medium is required for a sound wave.
- Physical quantities to describe a sound wave: displacement, strain and pressure.
- Longitudinal (compressional) vs. shear (transverse).

Basics of Acoustic Waves

- Longitudinal Wave:

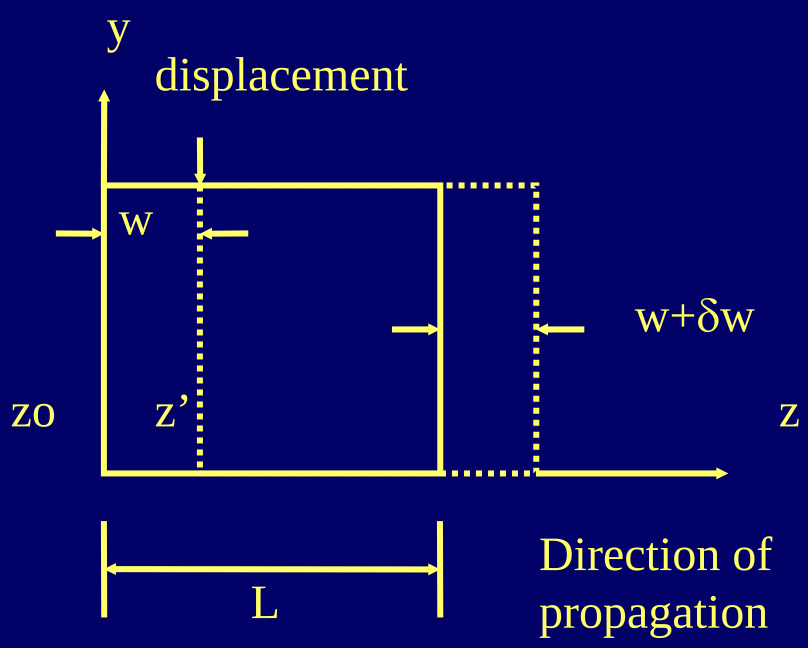

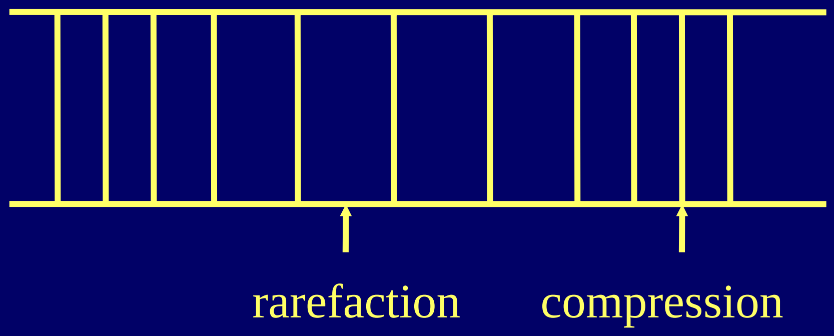

Basics of Acoustic Waves

- Shear Wave:

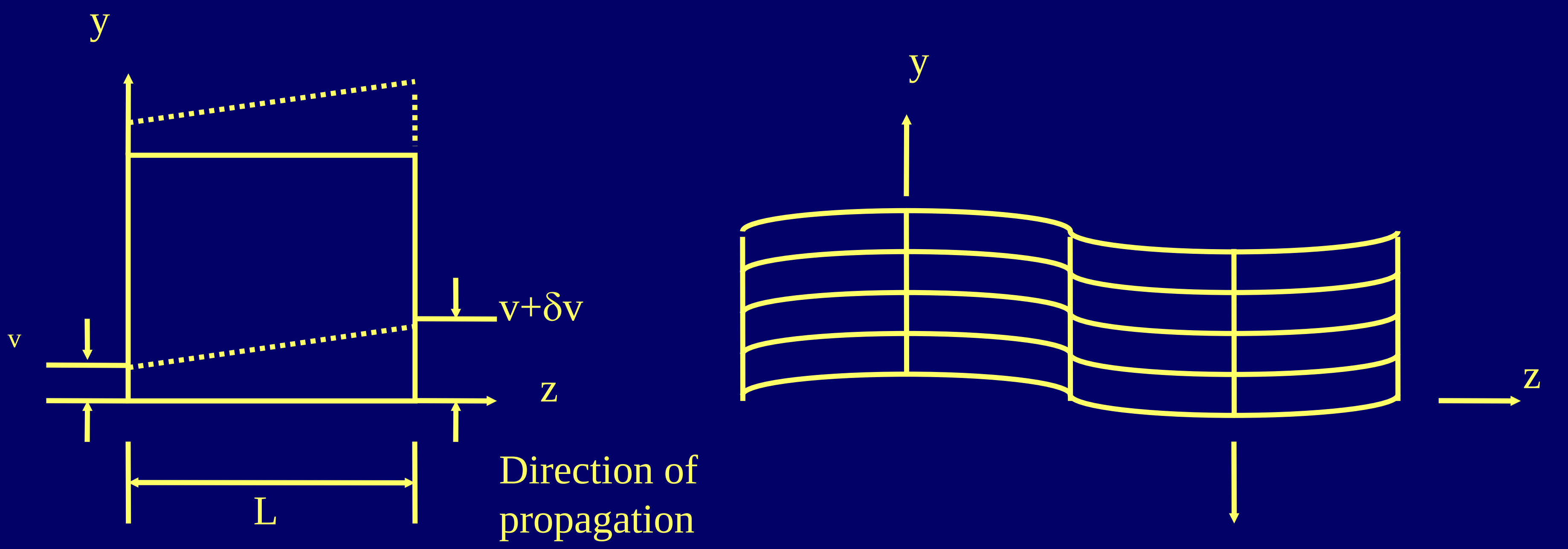

Basics of Acoustic Waves

- Longitudinal Wave:

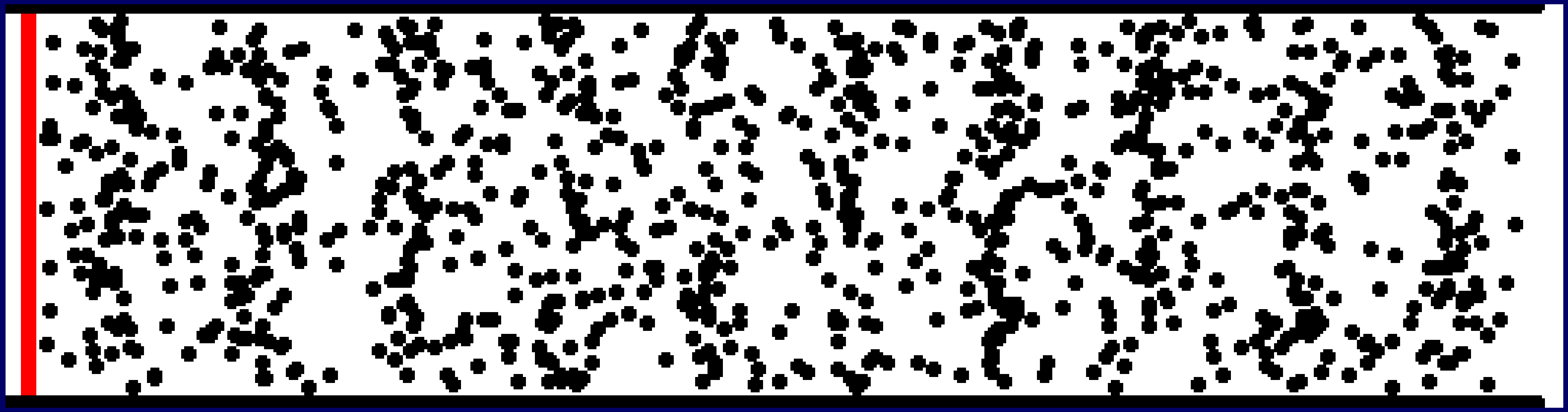

Basics of Acoustic Waves

- Shear Wave:

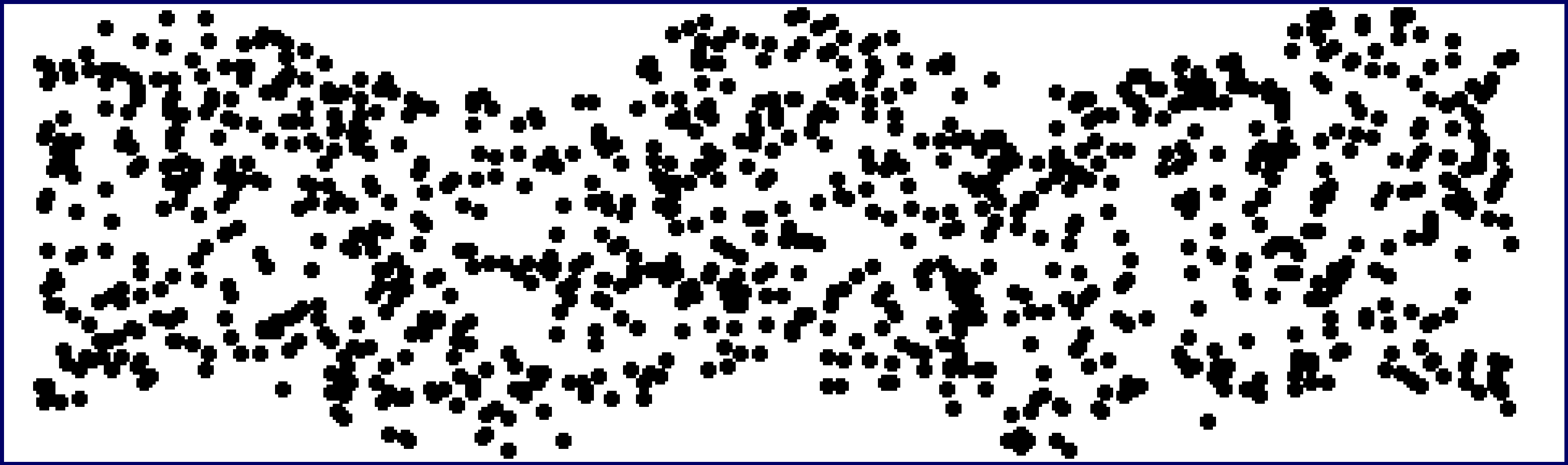

Displacement and Strain

- Displacement: movement of a particular point.
- Strain:
  - Displacement variations as a function of position.
  - Fractional change in length.
  - Deformation.
  - Can be extended to volume change.

Displacement and Strain

- Compressional strain:

$$\delta w = \frac{\partial w}{\partial z} L \equiv SL$$

$$S \equiv \frac{\partial w}{\partial z}$$

- Shear strain:

$$S \equiv \frac{\partial v}{\partial z}$$

Stress (Pressure)

- Force per unit area applied to the object.
- Net force applied to a unit volume:

$$\partial T \,/\, \partial z$$

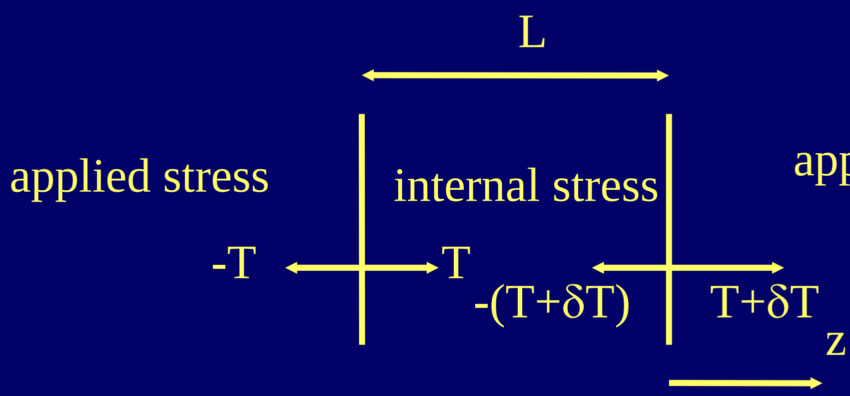

compressional stress

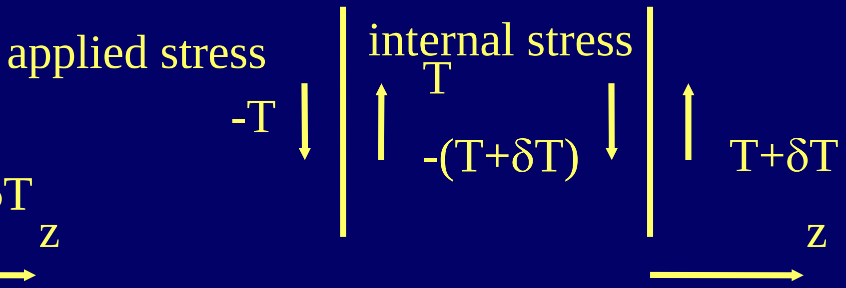

shear stress

Hooke's Law

- $T = cS$, where c is the elastic constant.
- Tensor representation:

Tensor notation	Reduced notation
xx	1
yy	2
zz	3
yz=zy	4
zx=xz	5
xy=yx	6

Hooke's Law (General Form)

$$\begin{bmatrix} T_1 \\ T_2 \\ T_3 \\ T_4 \\ T_5 \\ T_6 \end{bmatrix} = \begin{bmatrix} c_{11} & c_{12} & c_{13} & c_{14} & c_{15} & c_{16} \\ c_{21} & c_{22} & c_{23} & c_{24} & c_{25} & c_{26} \\ c_{31} & c_{32} & c_{33} & c_{34} & c_{35} & c_{36} \\ c_{41} & c_{42} & c_{43} & c_{44} & c_{45} & c_{46} \\ c_{51} & c_{52} & c_{53} & c_{54} & c_{55} & c_{56} \\ c_{61} & c_{62} & c_{63} & c_{64} & c_{65} & c_{66} \end{bmatrix} \begin{bmatrix} S_1 \\ S_2 \\ S_3 \\ S_4 \\ S_5 \\ S_6 \end{bmatrix}$$

- Stress tensor symmetry: no rotation.
- Strain tensor symmetry: by definition.

Hooke's Law (Isotropy)

$$\begin{bmatrix} T_1 \\ T_2 \\ T_3 \\ T_4 \\ T_5 \\ T_6 \end{bmatrix} = \begin{bmatrix} c_{11} & c_{12} & c_{12} & 0 & 0 & 0 \\ c_{12} & c_{11} & c_{12} & 0 & 0 & 0 \\ c_{12} & c_{12} & c_{11} & 0 & 0 & 0 \\ 0 & 0 & 0 & c_{44} & 0 & 0 \\ 0 & 0 & 0 & 0 & c_{44} & 0 \\ 0 & 0 & 0 & 0 & 0 & c_{44} \end{bmatrix} \begin{bmatrix} S_1 \\ S_2 \\ S_3 \\ S_4 \\ S_5 \\ S_6 \end{bmatrix}$$

$$c_{11} = c_{12} + 2c_{44} = \lambda + 2\mu$$

- Lamé constants: λ and μ (shear modulus).

Common Elastic Constants

- Young's modulus (elastic modulus, E):

$$T_{zz} = (\lambda + 2\mu) S_{zz} + \lambda (S_{xx} + S_{yy})$$

$$= \lambda (S_{xx} + S_{yy} + S_{zz}) + 2\mu S_{zz}$$

$$\equiv \lambda\Delta + 2\mu S_{zz}$$ (△: dilation)

$$E \equiv \frac{T_{zz}}{S_{zz}} = \frac{\mu(3\lambda + 2\mu)}{\lambda + \mu}$$

$E \approx 3\mu$ for liquid and soft tissues

Common Elastic Constants

- Bulk modulus (reciprocal of compressibility, B):

$$B \equiv -\frac{p}{\delta V / V} = -\frac{p}{\Delta}$$

$$p \equiv -\frac{\left(T_{xx} + T_{yy} + T_{zz}\right)}{3} = -B \cdot \Delta$$

$$B = \frac{3\lambda + 2\mu}{3}$$

Common Elastic Constants

- Poisson ratio (negative of the ratio of the transverse compression to the longitudinal compression, σ):

$$\sigma \equiv -\frac{S_{yy}}{S_{zz}} = \frac{\lambda}{2(\lambda+\mu)}$$

- σ approaches to 0.5 for liquid and soft tissues.

Acoustic Wave Equations

- Electrical and mechanical analogy:

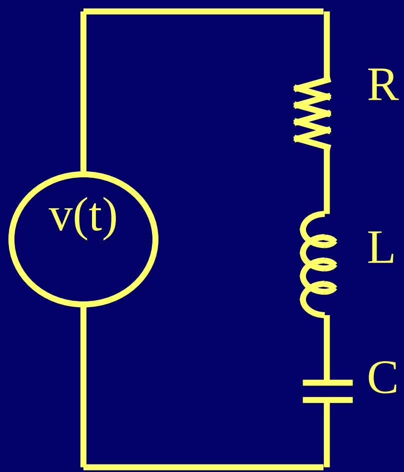

electrical

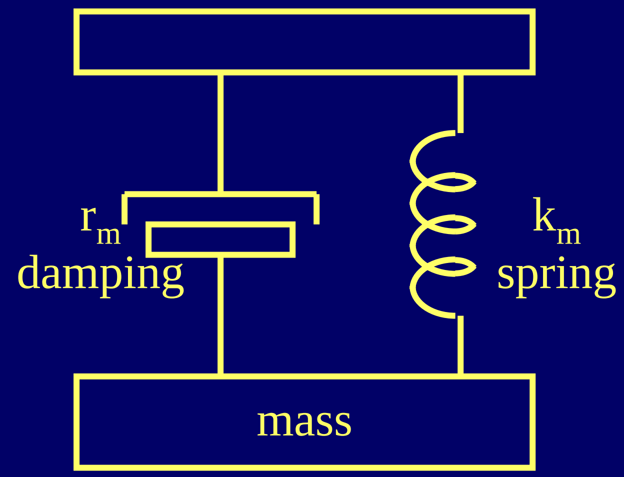

mechanical

Acoustic Wave Equations

$$L\frac{d^2q}{dt^2} + R\frac{dq}{dt} + \frac{q}{C} = v(t) \longleftrightarrow m\frac{d^2w}{dt^2} + r_m\frac{dw}{dt} + k_m w = f(t)$$

Electrical		Mechanical	
q	charge	w	displacement
$i=dq/dt$	current	$U=dw/dt$	particle velocity
V	voltage	f	force (stress, pressure)
L	inductance	m	mass
$1/C$	1/capacitance	k_m	stiffness
R	resistance	r_m	damping

Acoustic Wave Equations

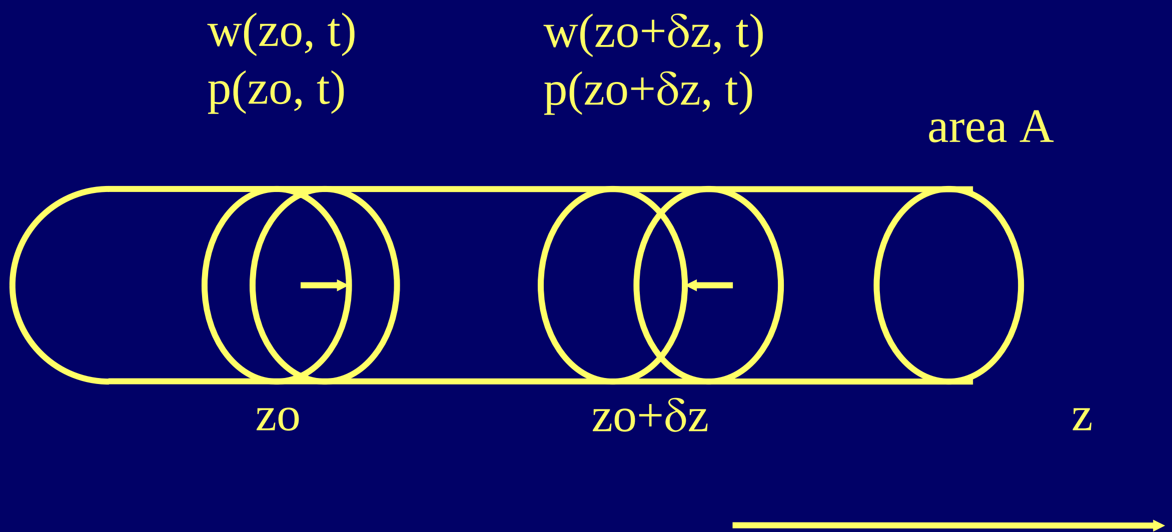

- Newton's second law:

$$A(p(z,t) - p(z+\delta z,t)) = (\rho \cdot \delta z \cdot A)\frac{\partial^2 w(z,t)}{\partial t^2}$$

$$\frac{\partial^2 w(z,t)}{\partial t^2} = (B/\rho)\frac{\partial^2 w(z,t)}{\partial z^2} \qquad c = \sqrt{B/\rho}$$

Acoustic Wave Equations

$$w(z,\omega) = w_1(\omega)\, e^{-j\omega z/c} + w_2(\omega)\, e^{j\omega z/c}$$

$$w(z,t) = w_1(t - z/c) + w_2(t + z/c)$$

$$u(z,t) \equiv \partial w(z,t)/\partial t$$

$$u(z,\omega) = j\omega w(z,\omega)$$

$$u(z,\omega) = u_1(\omega)\, e^{-j\omega z/c} + u_2(\omega)\, e^{j\omega z/c}$$

$$p(z,\omega) = -\frac{B}{j\omega}\frac{\partial u(z,\omega)}{\partial z}$$

$$= Z_0(u_1(\omega)e^{-j\omega z/c} - u_2(\omega)e^{j\omega z/c})$$

Characteristic impedance: $Z_0 = \rho c$

Two Common Units

- Pa (Pascal, pressure) :

$$1Pa = 1N / m^2 = 1Kg /(m \cdot \sec^2)$$

- Rayl (acoustic impedance) :

$$1Rayl = 1Pa /(m / \sec) = 1Kg /(m^2 \cdot \sec)$$

Reflection and Refraction

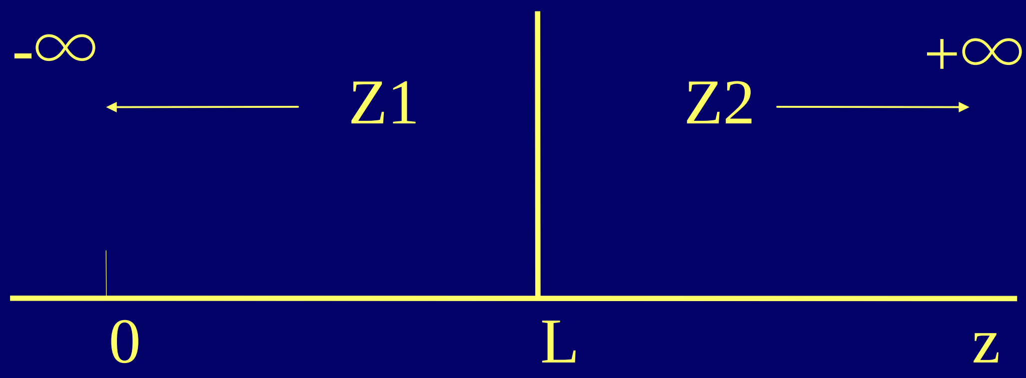

$$Z(z,\omega) \equiv \frac{p(z,\omega)}{u(z,\omega)} = Z_0 \frac{u_1(\omega)e^{-j\omega z/c} - u_2(\omega)e^{j\omega z/c}}{u_1(\omega)e^{-j\omega z/c} + u_2(\omega)e^{j\omega z/c}}$$

Reflection and Transmission

- 1D:

$$R_c = \frac{Z_2 - Z_1}{Z_2 + Z_1} (reflection)$$

$$T_c = \frac{2Z_2}{Z_2 + Z_1} (transmission)$$

Reflection

Hard Boundary

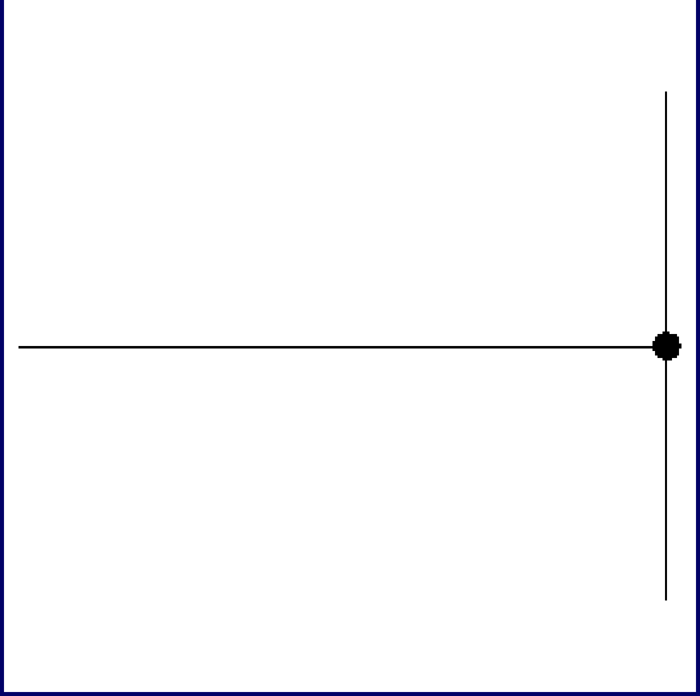

Soft Boundary

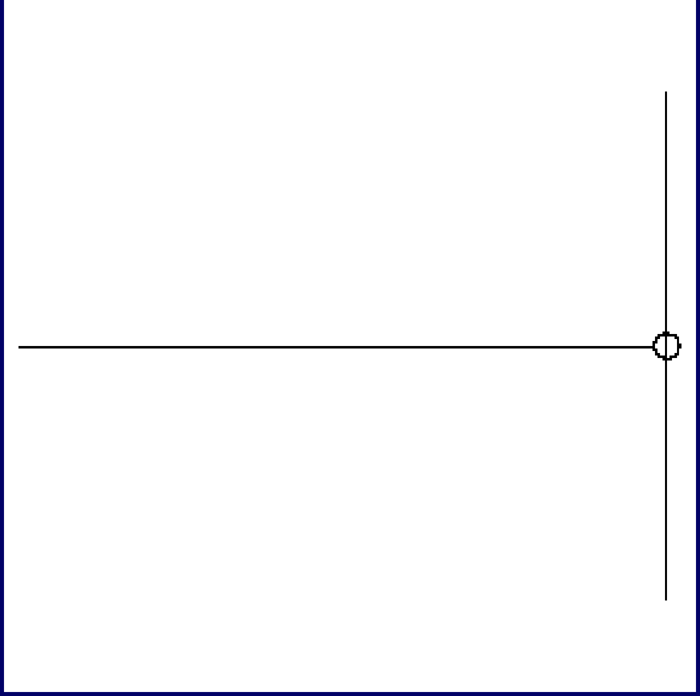

Reflection

Low Density to High Density

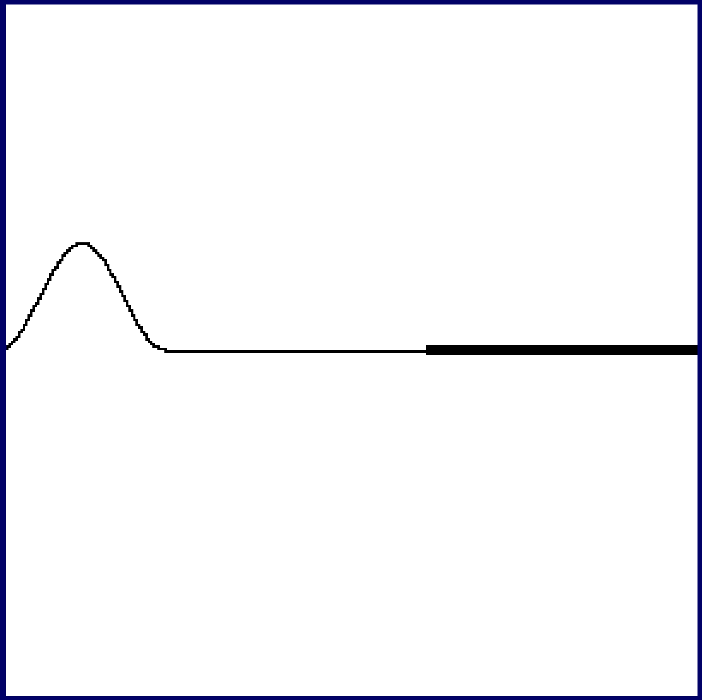

High Density to Low Density

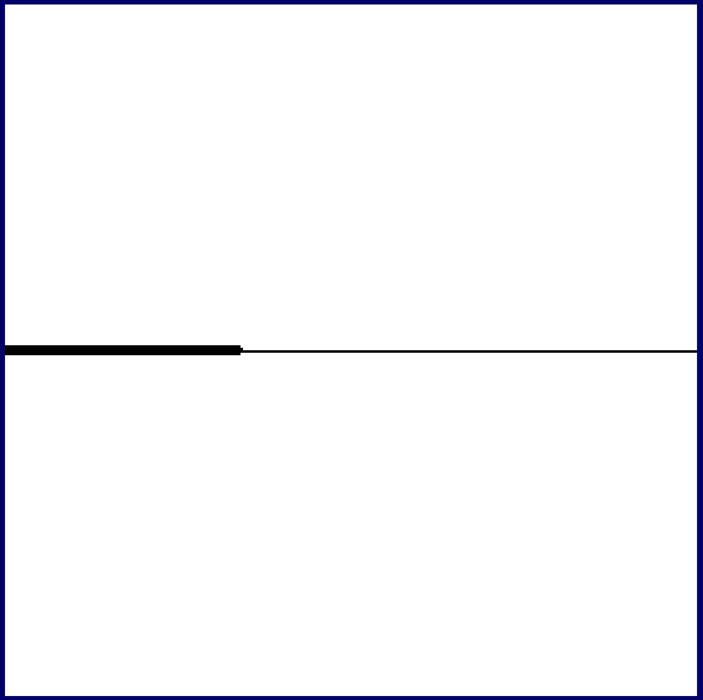

Reflection, Transmission and Refraction

- 2D:

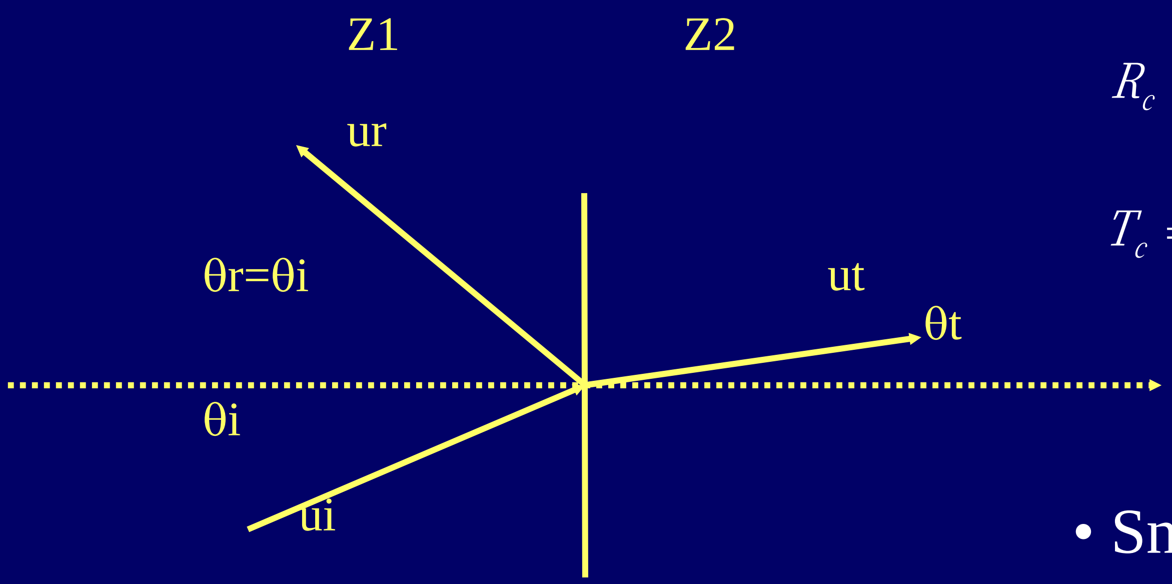

$$R_c = \frac{Z_2 \cos\theta_i - Z_1 \cos\theta_t}{Z_2 \cos\theta_i + Z_1 \cos\theta_t} (\,reflection\,)$$

$$T_c = \frac{2Z_2 \cos\theta_i}{Z_2 \cos\theta_i + Z_1 \cos\theta_t} (\,transmission\,)$$

- Snell's law: $\dfrac{\sin\theta_i}{\sin\theta_t} = \dfrac{c_1}{c_2}$

- Critical angle, if $c_1 \geq c_2$: $\theta_{ic} \equiv \sin^{-1}(c_1 / c_2)$

Refraction

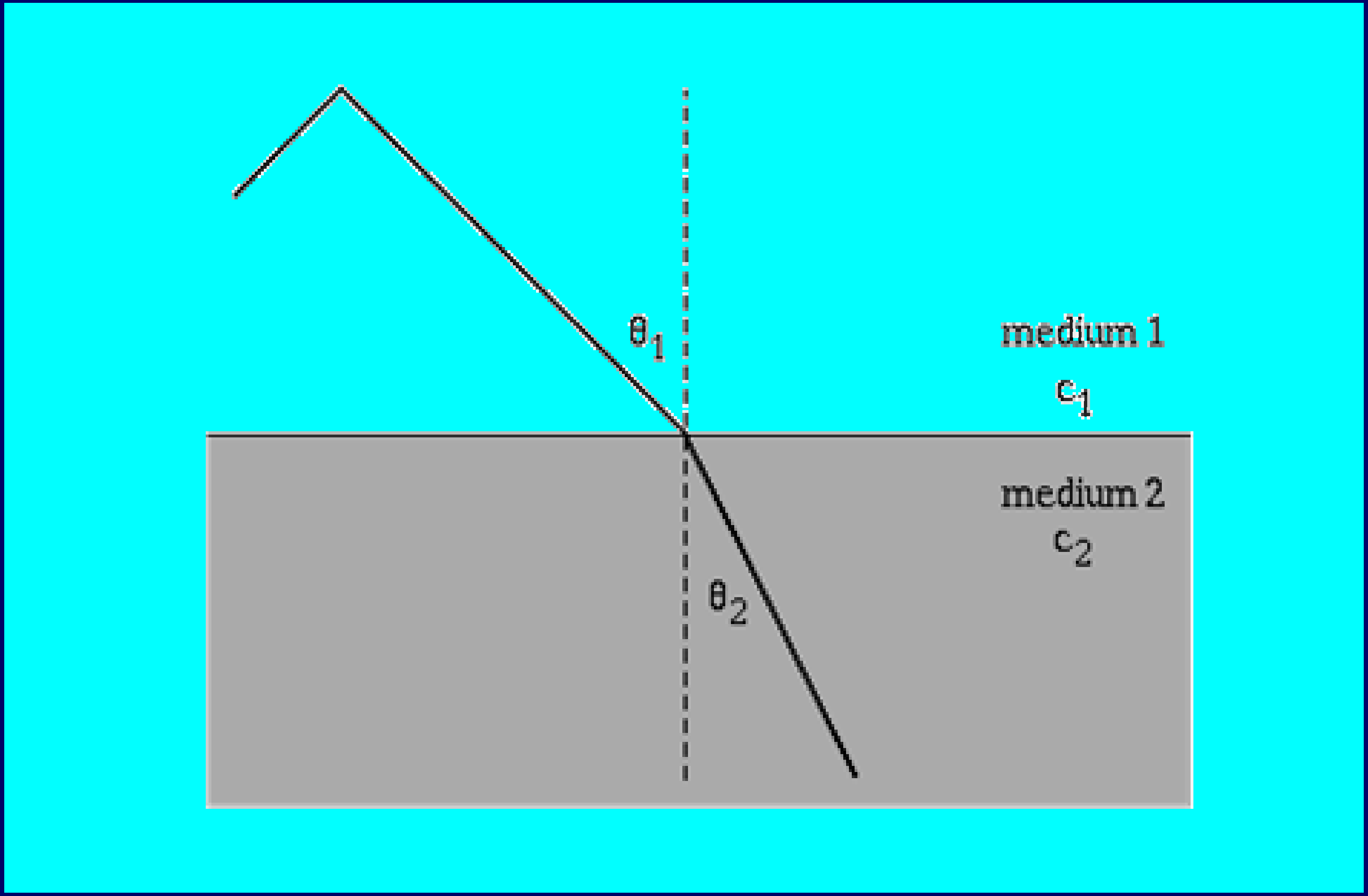

Table IV
Velocity and acoustic impedance of pertinent materials and biological tissues at room temperature (20–25°C)

	Velocity (m/sec)	Impedance $\times 10^{-6}$ (kg/m²-sec)[a]
Water	1484	1.48
Aluminum	6420	17.00
Air	343	0.0004
Plexiglas	2670	3.20
Blood	1550	1.61
Myocardium (perpendicular to fibers)	1550	1.62
Fat	1450	1.38
Liver	1570	1.65
Kidney	1560	1.62
Skull bone	3360 (longitudinal)	6.00

[a] Rayl is a unit commonly used for acoustic impedance. One rayl = 1 kg/m²-sec.

TABLE 9.3

REFLECTIVITY OF NORMALLY INCIDENT WAVES

Materials at Interface	Reflectivity
Brain–skull bone	0.66
Fat–bone	0.69
Fat–blood	0.08
Fat–kidney	0.08
Fat–muscle	0.10
Fat–liver	0.09
Lens–aqueous humor	0.10
Lens–vitreous humor	0.09
Muscle–blood	0.03
Muscle–kidney	0.03
Muscle–liver	0.01
Soft tissue (mean value)–water	0.05
Soft tissue–air	0.9995
Soft tissue–PZT5 crystal	0.89

Scattering, Attenuation and Speckle

Scattering

Histology

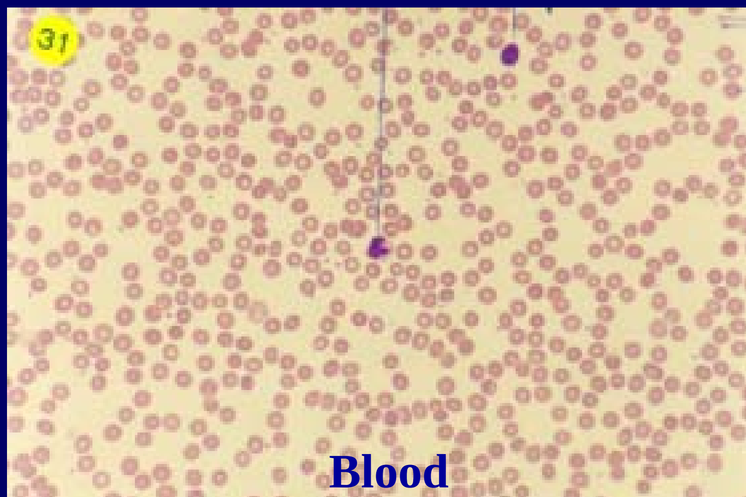

Blood

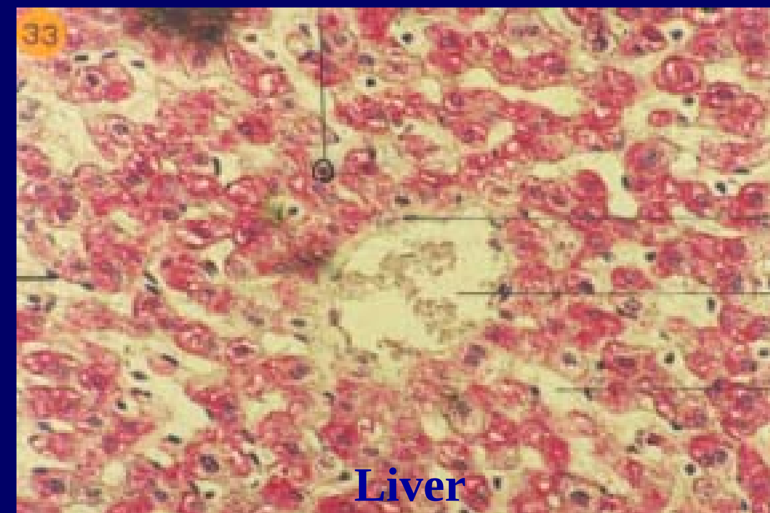

Liver

Kidney

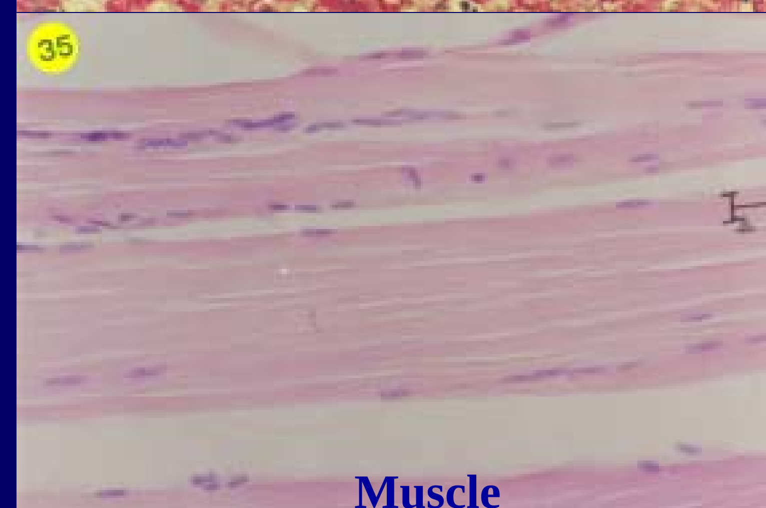

Muscle

Reflection vs. Scattering

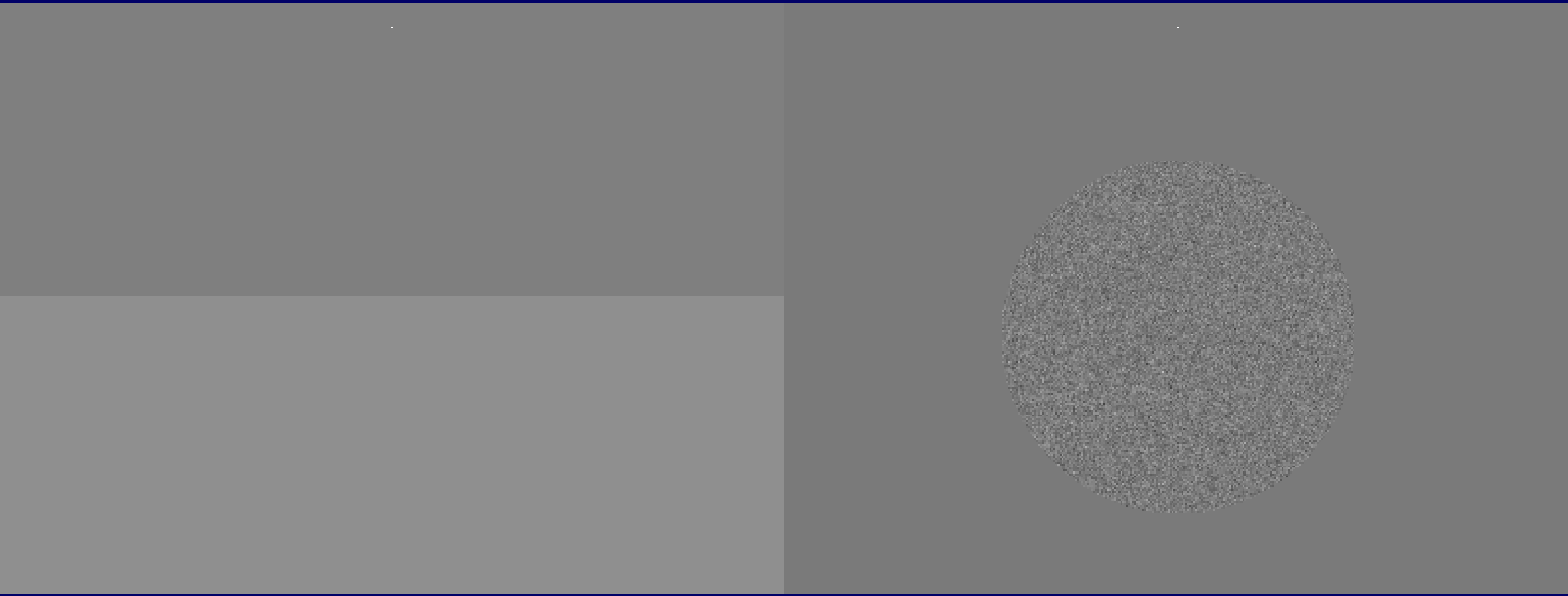

Scattering

- (*Specular*) Relfection vs. (*Rayleigh*) Scattering.
- Angular scattering vs. Back-scattering.

- Optical : $ka>>1$
- Rayleigh : $ka<<1$.
- Oscillatory : in between.

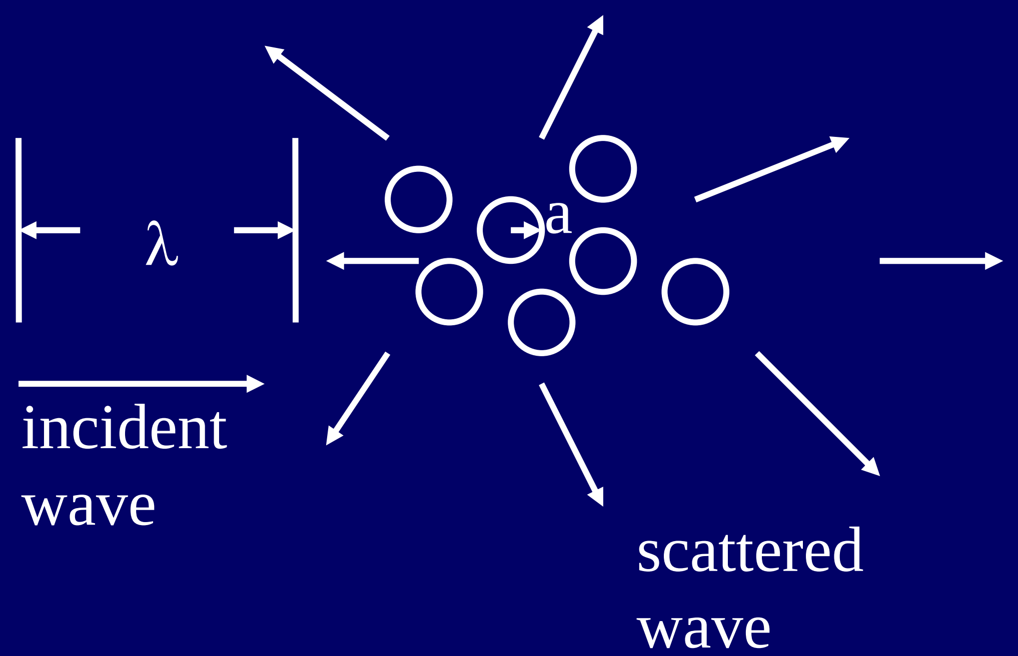

Scatter Parameters

- Scatter cross section (σ_s):
  - Total scattered power/Incident energy.
- Backscatter cross section (σ_b).
- Backscatter coefficient (ε):
  - σ_b per unit volume of scatterers.
  - ε normalized to solid angle (sr^{-1}).

Scattering Properties

- Rayleigh scattering (ignoring secondary scattering):

$$\sigma_s \propto k^4 a^6$$

- Determing factors:
  - Size and structure.
  - Cell, blood vessel and ductal network.
- Roughly Speaking:
  - Blood: f^4.
  - Myocardium: f^3.
  - Other soft tissue: $f^{1.5\text{-}2.5}$.

Scattering Properties

Frequency (MHz)	$\varepsilon(mm^{-1})$ heart tissue	$\varepsilon(mm^{-1})$ blood
2.5	4.3×10^{-5}	0.5×10^{-6}
3.75	1.5×10^{-4}	2.6×10^{-6}
5.0	5.0×10^{-4}	8.2×10^{-6}

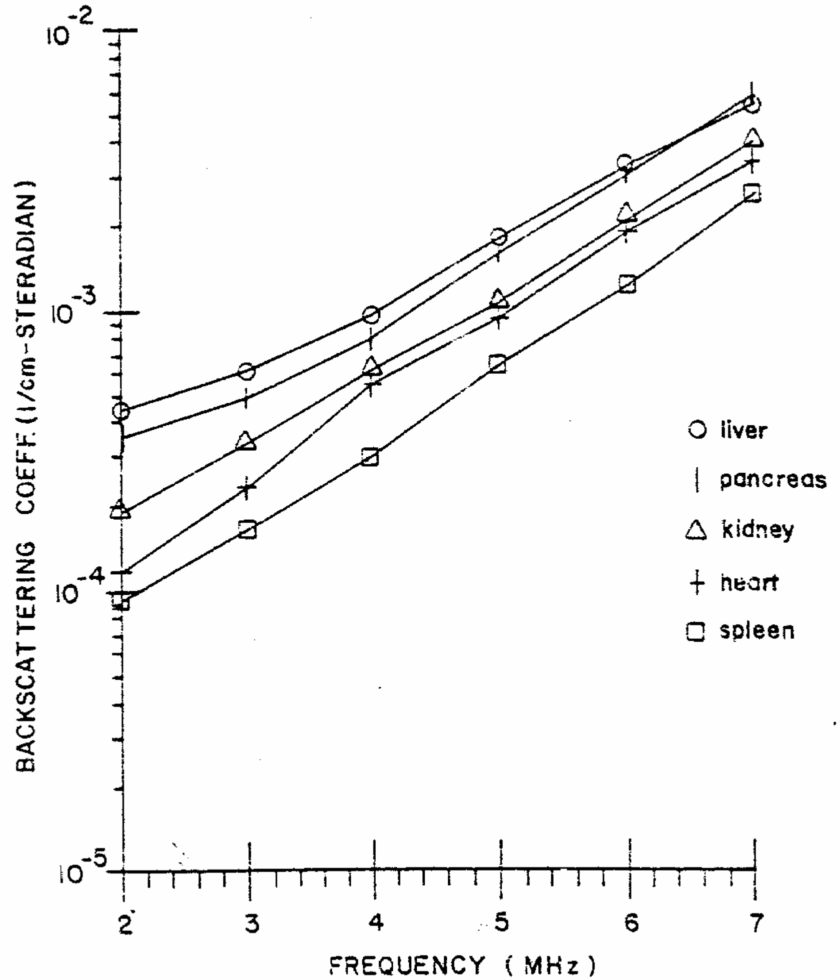

Figure 75 Backscattering coefficient of bovine tissues as a function of frequency.

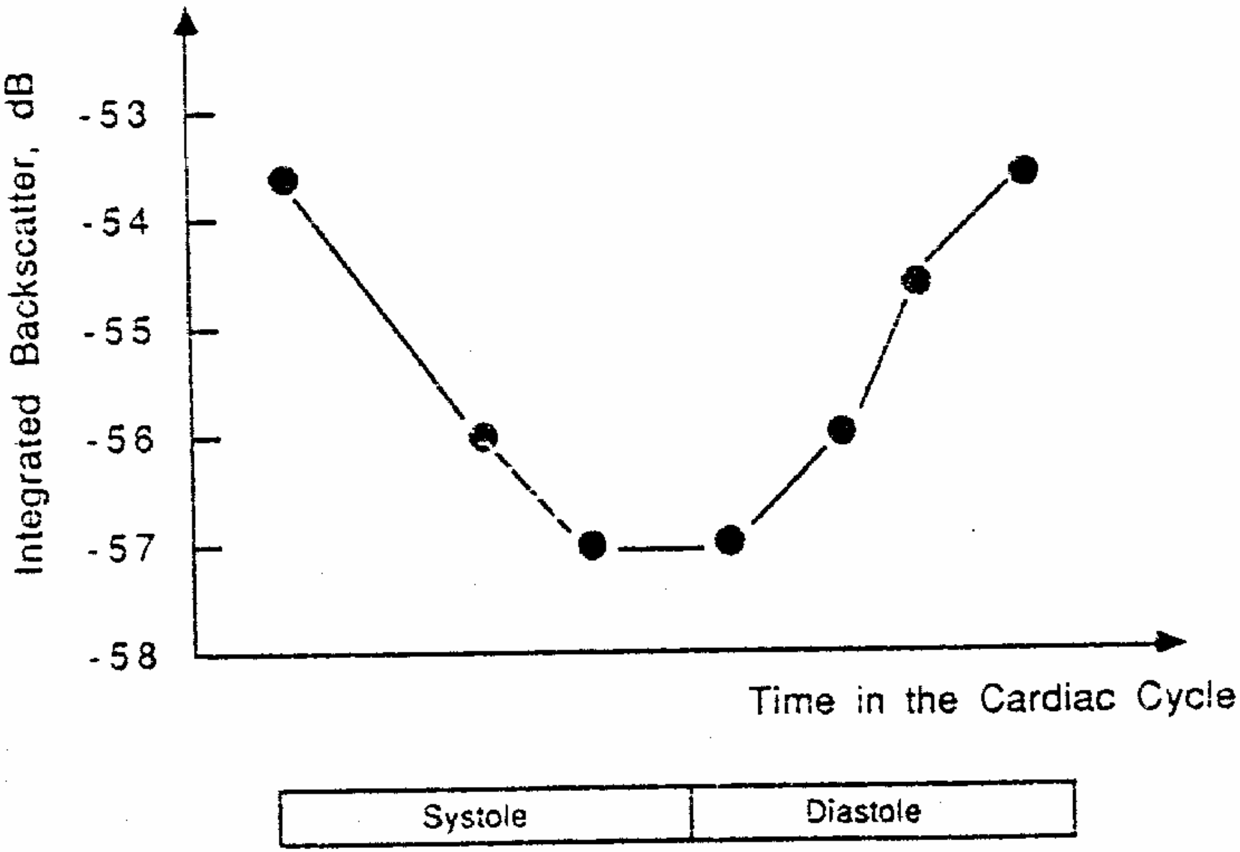

Figure 77 Integrated backscatter defined as the averaged backscatter coefficient over a frequency band relative to that from a flat reflector of canine myocardium measured *in vivo* as a function of cardiac cycle. (From Miller *et al.*, 1985).

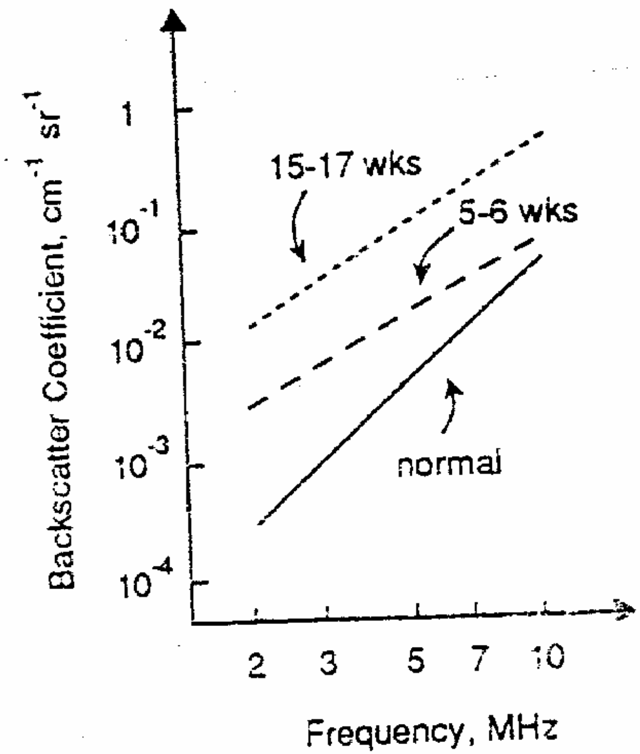

Figure 76 Backscattering coefficient of canine myocardium as a function of frequency. Solid line, normal; dashed line, 5–6 weeks after coronary occlusion; dotted line, 15–17 weeks after coronary occlusion. (From O'Donnell *et al.*, 1981).

Attenuation

Attenuation

- Sources of energy loss:
  - Reflection and scattering.
  - Relaxation.
- Relaxation:
  - Pressure change and volume change are not in phase.
  - Product of absorption and wavelength are roughly constant.
- Fundamental limitations of penetration:
  - Attenuation.
  - Safety requirements.

Attenuation

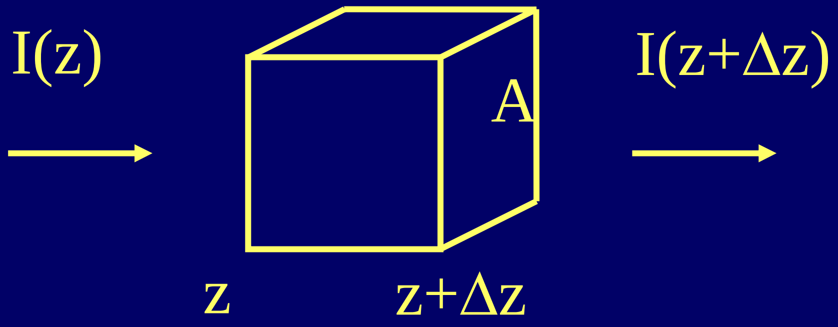

$$A \cdot I(z+\Delta z) = A \cdot I(z) - 2\beta A \cdot I(z)\Delta z$$

$$-\frac{\partial I(z)}{\partial z} = 2 \cdot \beta I(z)$$

$$I(z) = I_0 e^{-2\beta z}$$

$$\beta = \alpha f$$

Attenuation

$$H(z,f) = e^{-(\alpha f z + j2\pi f z / c)}$$

$$I(z,f) = I_0 \left| H(z,f) \right|^2 = I_0 e^{-2\alpha f z}$$

$$-10\log_{10}\left(\frac{I(z,f)}{I_0}\right) = 20(\log_{10} e)\alpha f z = 8.69\alpha f z$$

$$\alpha_{dB} = 8.69\alpha_{nepers}.$$

Attenuation

- Assuming a Gaussian signal:

$$\left|S_t(f)\right|^2 = e^{-(\frac{f-f_0}{\sigma})^2}$$

$$\left|S_r(R,f)\right|^2 = \left|S_t(f)\right|^2 e^{-4\alpha Rf} = e^{-(\frac{f-f_0}{\sigma})^2 - 4\alpha Rf}$$

$$\left|S_r(R,f)\right|^2 = e^{-(\frac{f-f_1}{\sigma})^2} e^{-4\alpha R(f_0-\sigma^2\alpha R)}$$

$$f_1 = f_0 - 2\sigma^2\alpha R.$$

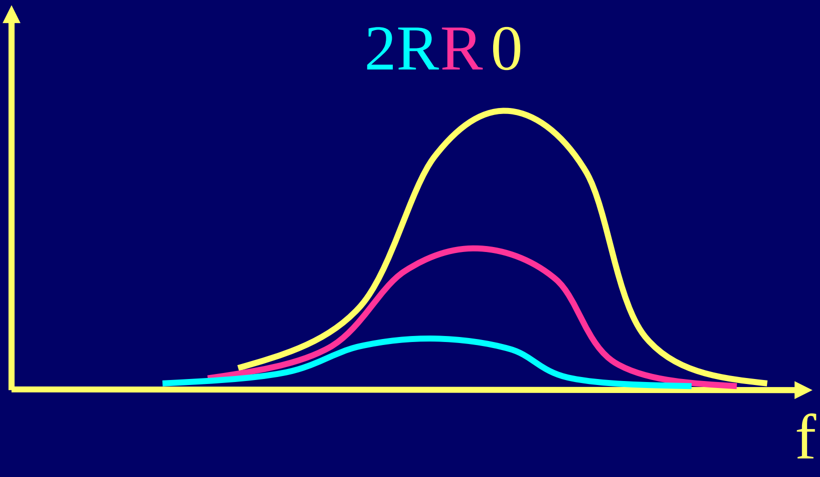

Attenuation on Pulse Shape

- Center frequency downshift → Lateral resolution decreases with depth.
- The downshift is proportional to:
  - Bandwidth^2.
  - Attenuation coefficient.
- Absolute bandwidth is un-changed → Axial resolution is un-affected.
- Tradeoff between lateral and axial resolution.

Table V
Attenuation coefficients of biological tissues and pertinent materials

Material	Attenuation coefficient (np/cm at 1 MHz at 20°C)
Air	1.38
Aluminum	0.0021
Plexiglas	0.23
Water	0.00025
Fat	0.06
Blood	0.02
Myocardium (perpendicular to fiber)	0.35
Liver	0.11
Kidney	0.09
Skull bone	1.30

Speckle


2:07:06 pm
8C4
H8.0MHz
75dB S1/+1/1/4
Gain= -6dB ∆=2


Works-in-Progress

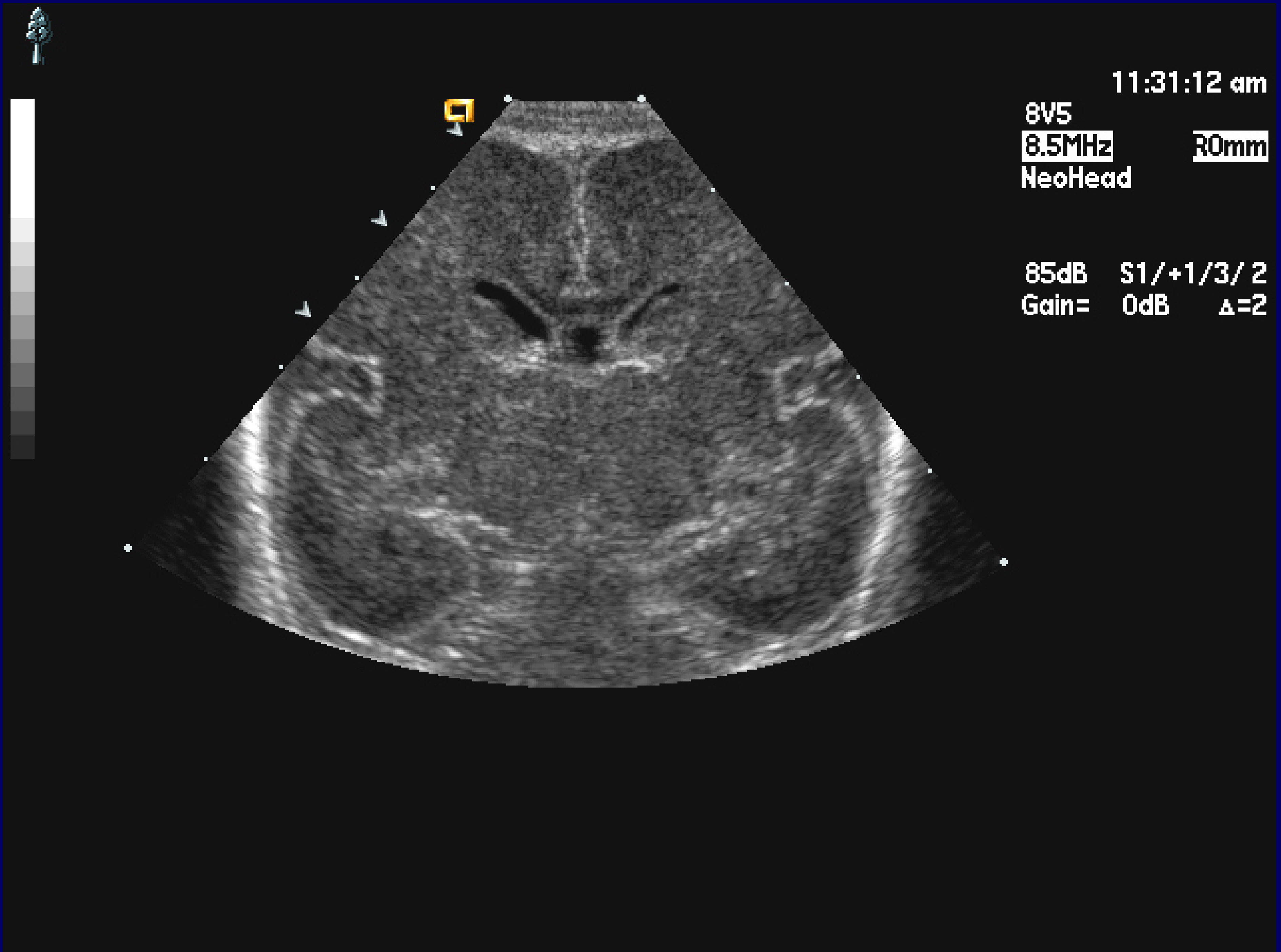

11:31:12 am
8V5
8.5MHz
80mm
NeoHead
85dB
S1/+1/3/ 2
Gain=
0dB
Δ=2

Speckle Formation

- Speckle results from coherent interference of un-resolvable objects.

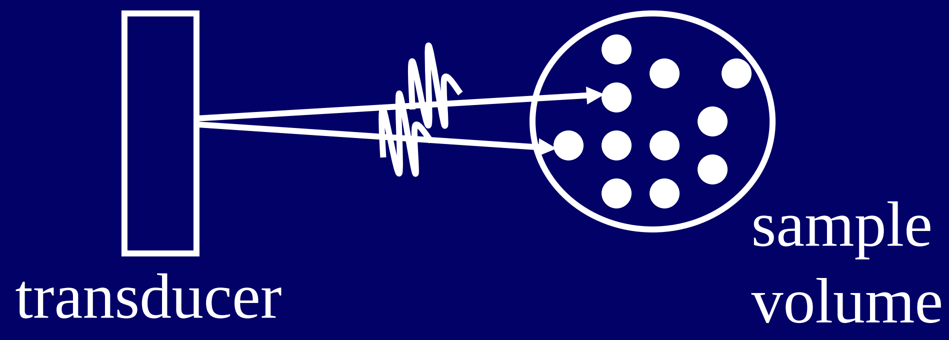

Speckle Formation

- In diagnostic ultrasound, the size of tissue micro-structures is often much smaller than a typical wavelength.
- Pulse-echo ultrasonic images are formed using the phase information.
- Speckle appears as brightness variations and obscure the underlying information.

Speckle Noise

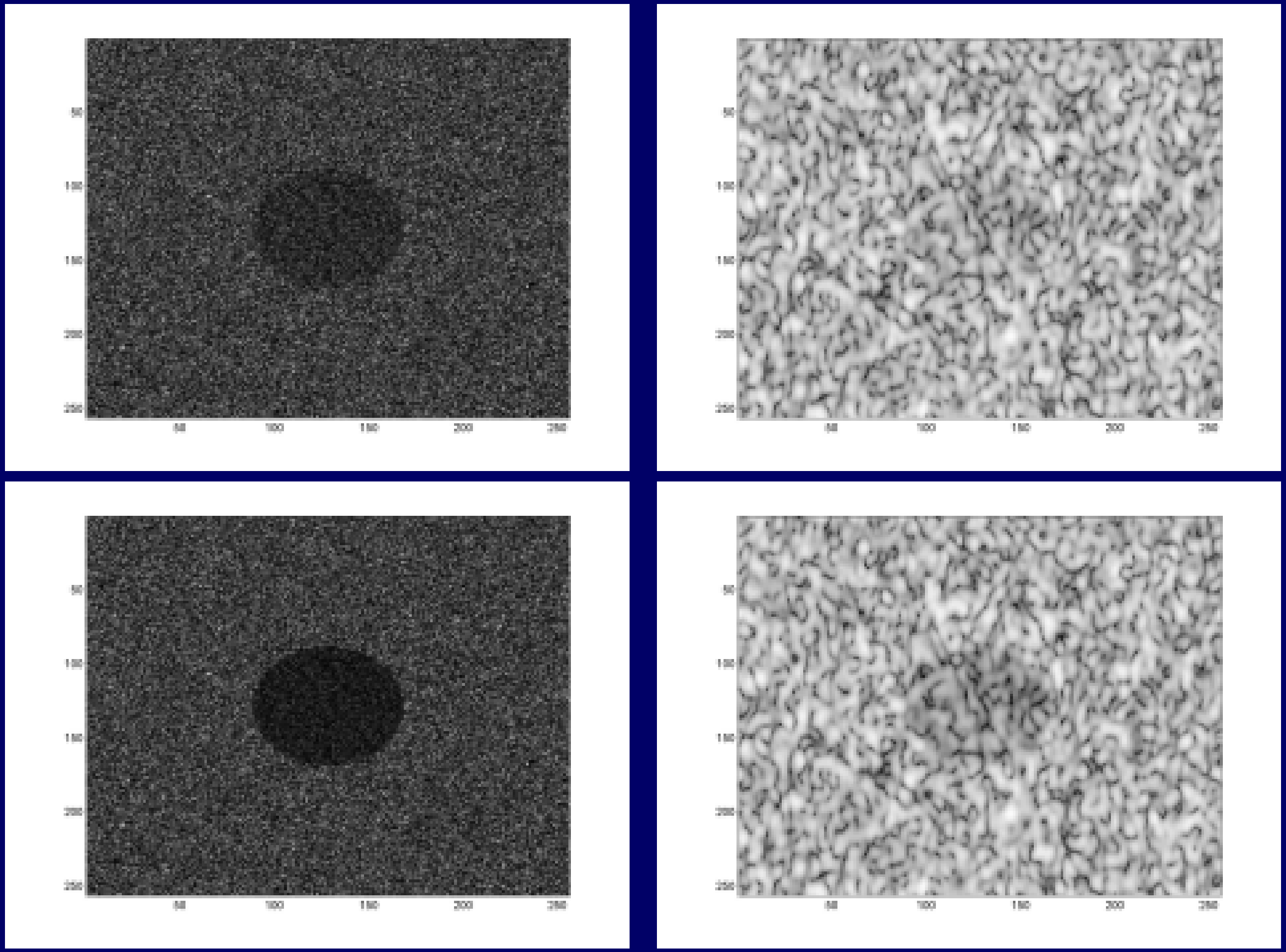

Speckle Noise

- Coherent sum of random signals from sound scatterers in a resolution cell.
- Brightness variations are independent of tissue properties.
- Multiplicative noise.
- Fundamental limitation of contrast resolution.

Speckle First-Order Statistics

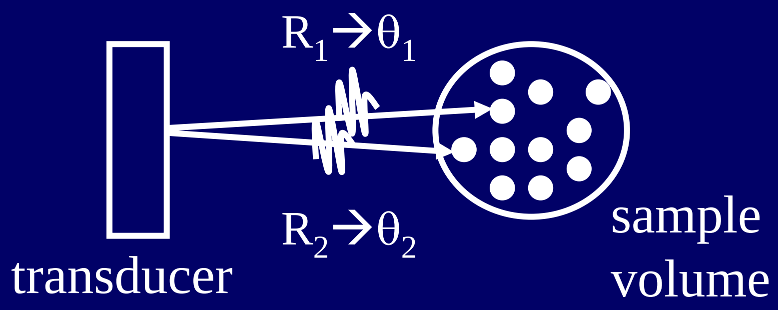

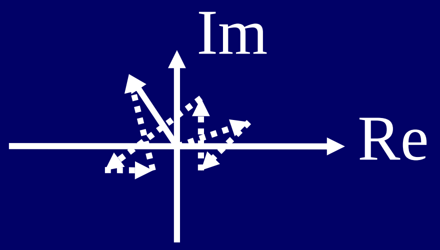

$$\mathrm{Re}\left\{A\right\} = \frac{1}{\sqrt{N}} \sum_{k=1}^{N} \left|a_k\right| \cos \theta_k$$

$$\mathrm{Im}\left\{A\right\} = \frac{1}{\sqrt{N}} \sum_{k=1}^{N} \left|a_k\right| \sin \theta_k$$

$$p_{\mathrm{Re}\{A\}.\mathrm{Im}\{A\}} = \frac{1}{2\pi\sigma^2} e^{-\frac{\mathrm{Re}\{A\}^2 + \mathrm{Im}\{A\}^2}{2\sigma^2}}$$

$$\sigma^2 = \frac{1}{N} \sum_{k=1}^{N} \frac{\left|a_k\right|^2}{2}$$

Speckle First-Order Statistics

$$p_I = \frac{1}{2\sigma^2} e^{-\frac{I}{2\sigma^2}}$$

$$p_E = \frac{E}{\sigma^2} e^{-\frac{E^2}{2\sigma^2}}$$

$$SNR_I \equiv \frac{\langle I \rangle}{\sigma_I} = 1$$

$$SNR_E \equiv \frac{\langle I \rangle}{\sigma_E} = \frac{\left(\pi\sigma^2/2\right)^{1/2}}{\left(\left(4-\pi\right)\sigma^2/2\right)^{1/2}} \approx 1.91$$

Speckle First-Order Statistics

- On a log display:

$$D(dB) = f(I) \equiv 10\log_{10}\left(\frac{I}{I_0}\right)$$

$$D = f(\langle I \rangle) + \left(I - \langle I \rangle\right) f'\left(\langle I \rangle\right) + R$$

$$\sigma_D{}^2 \approx f'(\langle I \rangle)^2 \sigma_I{}^2 = \left(\frac{10}{\ln 10}\right)^2 \frac{\sigma_I{}^2}{\langle I \rangle^2}$$

$$\sigma_D \approx 4.34(dB)$$

← Fundamental Limitation of Contrast Resolution

Speckle Noise

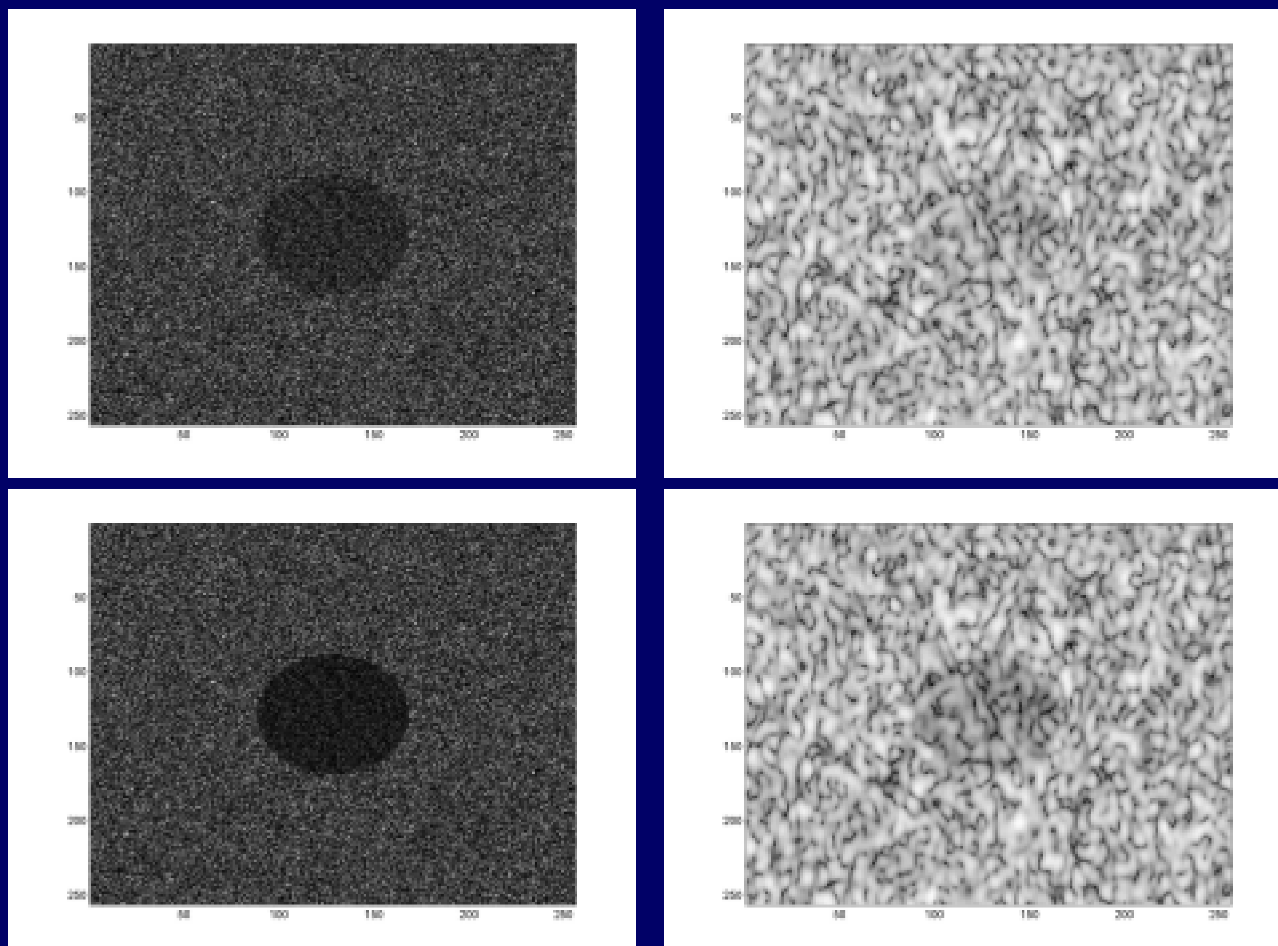

Optoacoustic Imaging: Theory and Principles [15]

Optoacoustic Pressure Production

$$p_{\mathbf{r}}(t) \approx \frac{\beta I_0 v_s}{4\pi C}\tau\frac{d}{dt}\oiint_{|\mathbf{r}-\mathbf{r}'|=v_s t} A(\mathbf{r}')\frac{d\mathbf{r}'}{v_s t},$$

- A laser pulse that is short enough such that thermal diffusion can be ignored.
- *A(***r'***)* is the fractional energy-absorption per-unit-volume of soft tissue at position **r'**.
- Integral of pressure waves over the surface of a sphere.

Example: Uniformly Absorbing Sphere

- 5 mm radius.

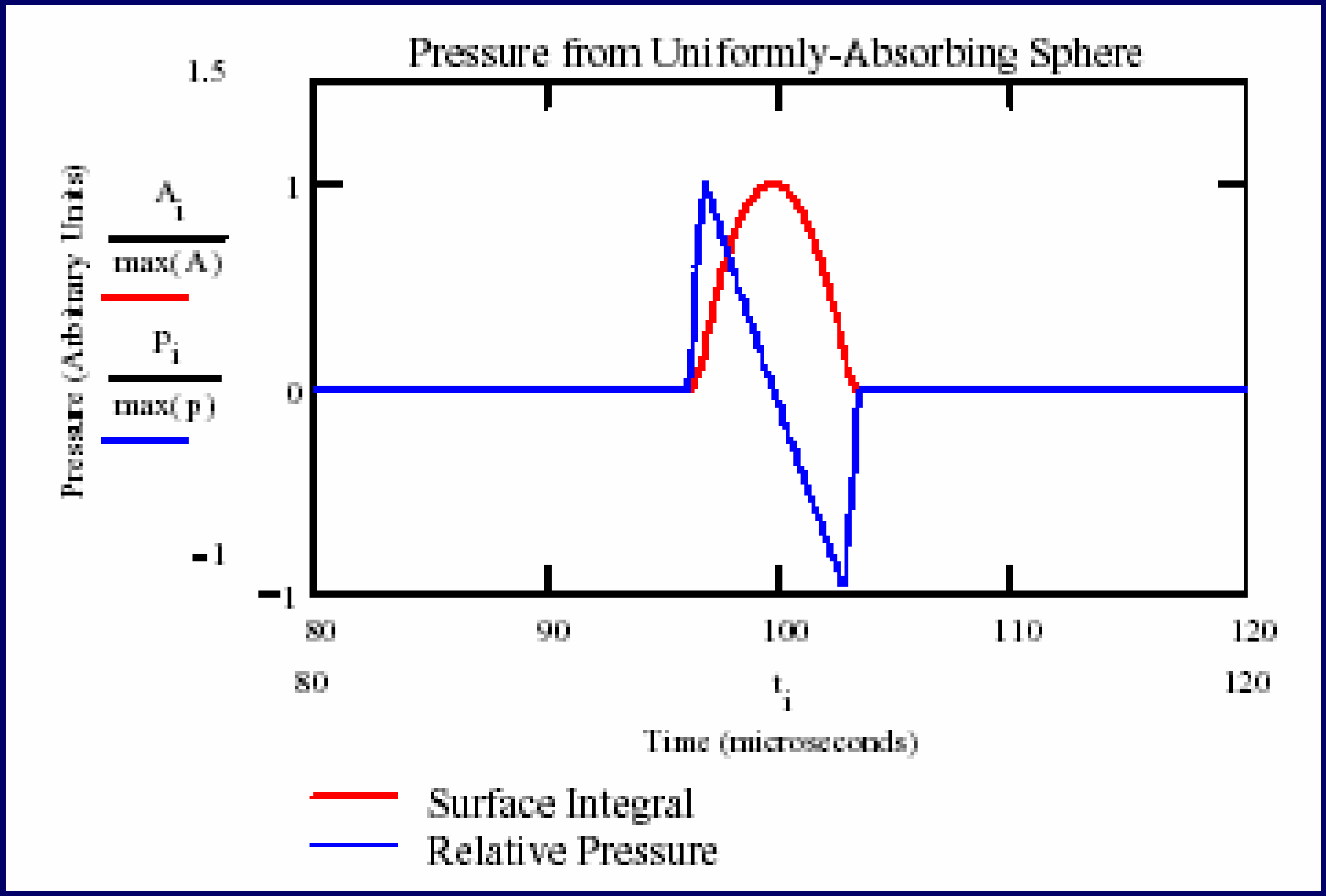

Image Reconstruction

- Objective: reconstruct *A(***r'***)* (contrast mechanism).
- Re-formulate as a Radon transform:

$$F_{\mathbf{r}}(t) \equiv \frac{4\pi C}{\beta I_0 \tau} t \int_0^t p_{\mathbf{r}}(t')\,dt' \approx \oiint_{|\mathbf{r}-\mathbf{r}'|/v_s = t} A(\mathbf{r}')\,d\mathbf{r}'$$

Projection

- Reconstruction → 3D inverse Radon transform.

3D Inverse Radon Transform

- Taking second spatial derivative of the projection (i.e., the first temporal derivative of the pressure).
- Back-projection.
- Integration over all projection directions.

Issues in Reconstruction

- If the distance is sufficiently larger than the object size, the spherical wave can be approximated as a planar wave.
- Due to the transducer's frequency response, filtered-backprojection is required.

$$p'_{\mathbf{r}}(t) = p_{\mathbf{r}}(t) * i_{\mathbf{r}}(t)$$

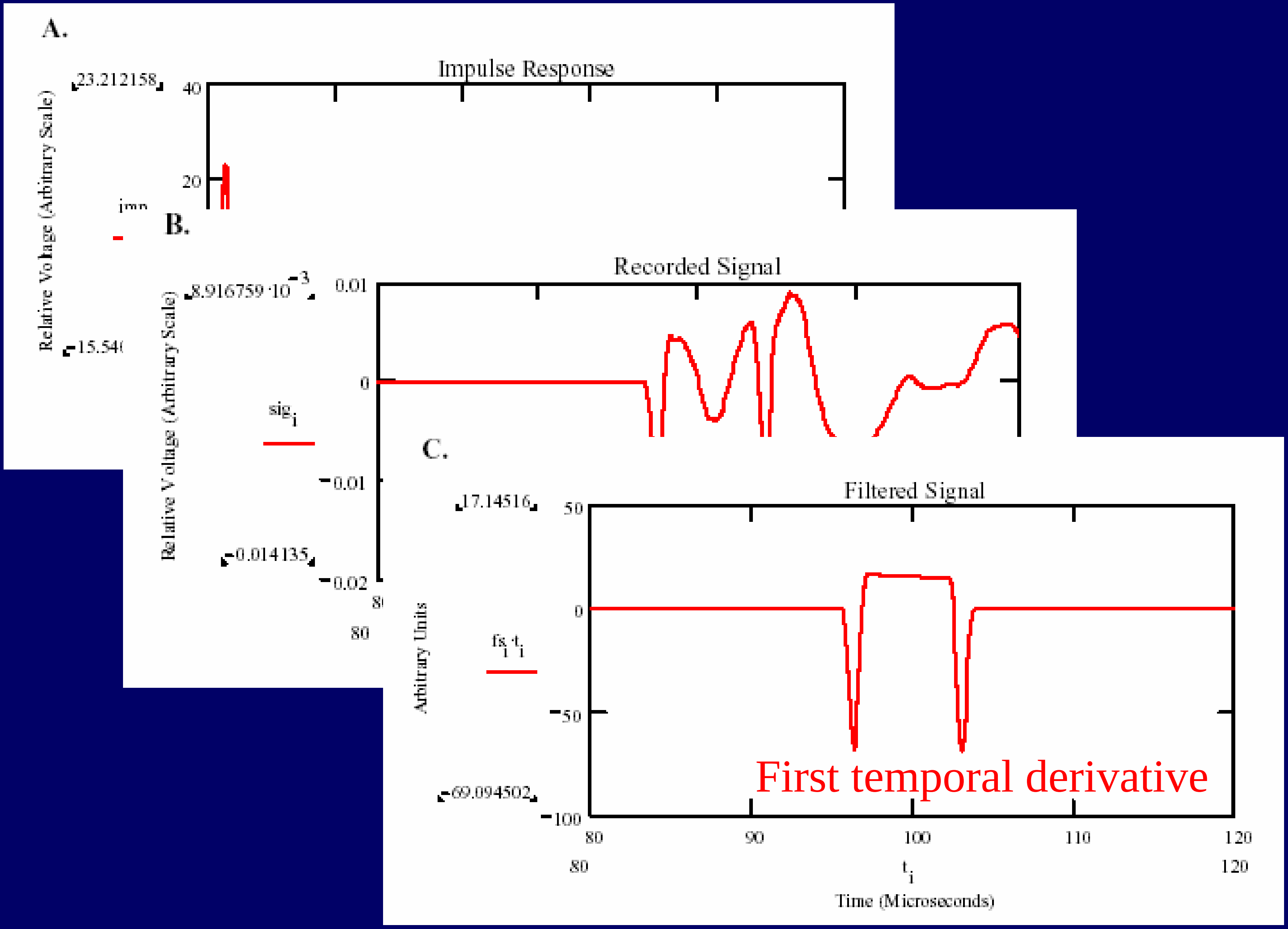
A.
Impulse Response
23.212158
40
20
Relative Voltage (Arbitrary Scale)
B.
Recorded Signal
8.916759·10⁻³
0.01
0
−0.01
−0.02
−0.014135
80
Relative Voltage (Arbitrary Scale)
C.
Filtered Signal
17.14516
50
0
−50
−100
−69.094502
Arbitrary Units
80
90
100
110
120
80
120
Time (Microseconds)
First temporal derivative

Imaging Setup

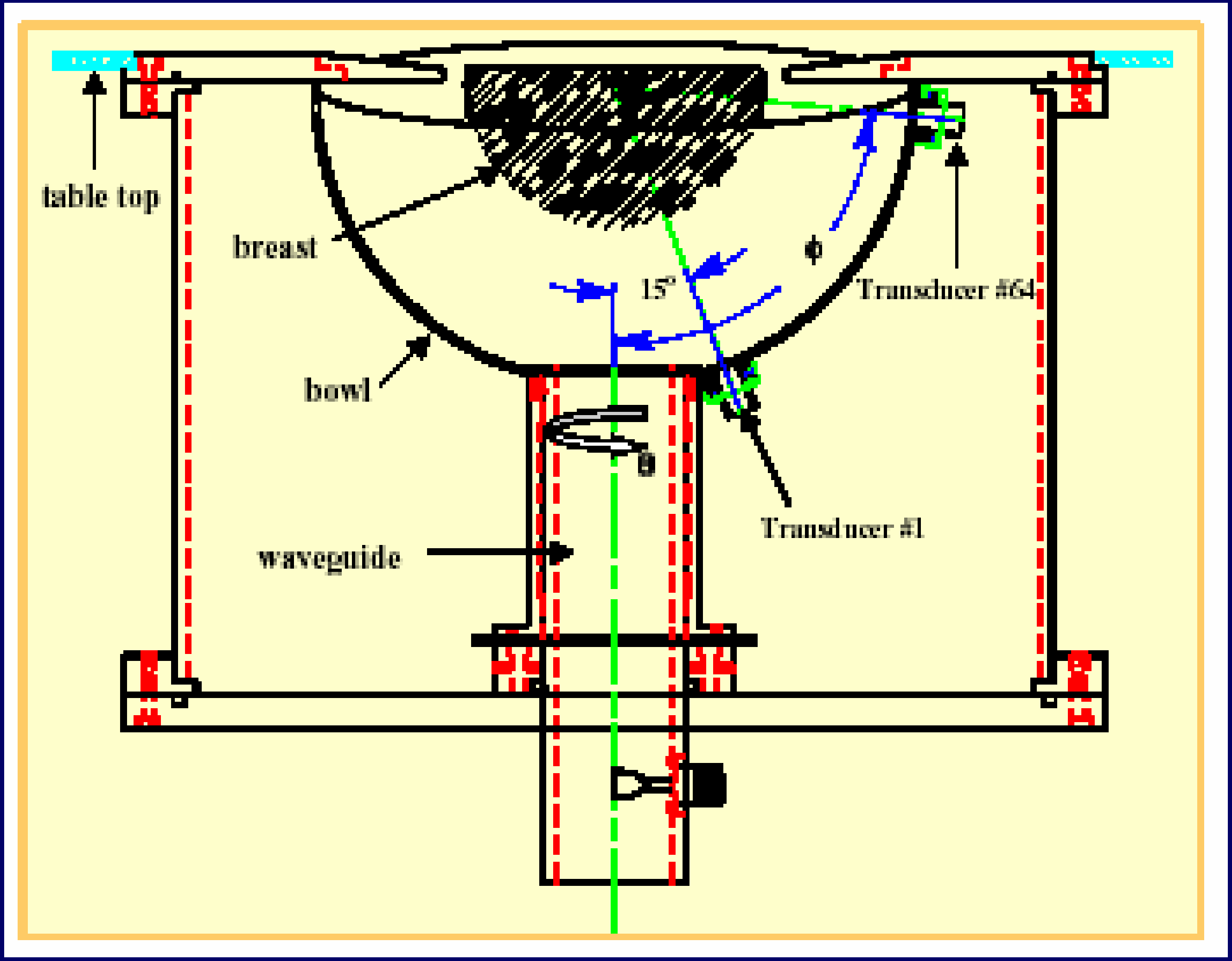

A Simulation Example

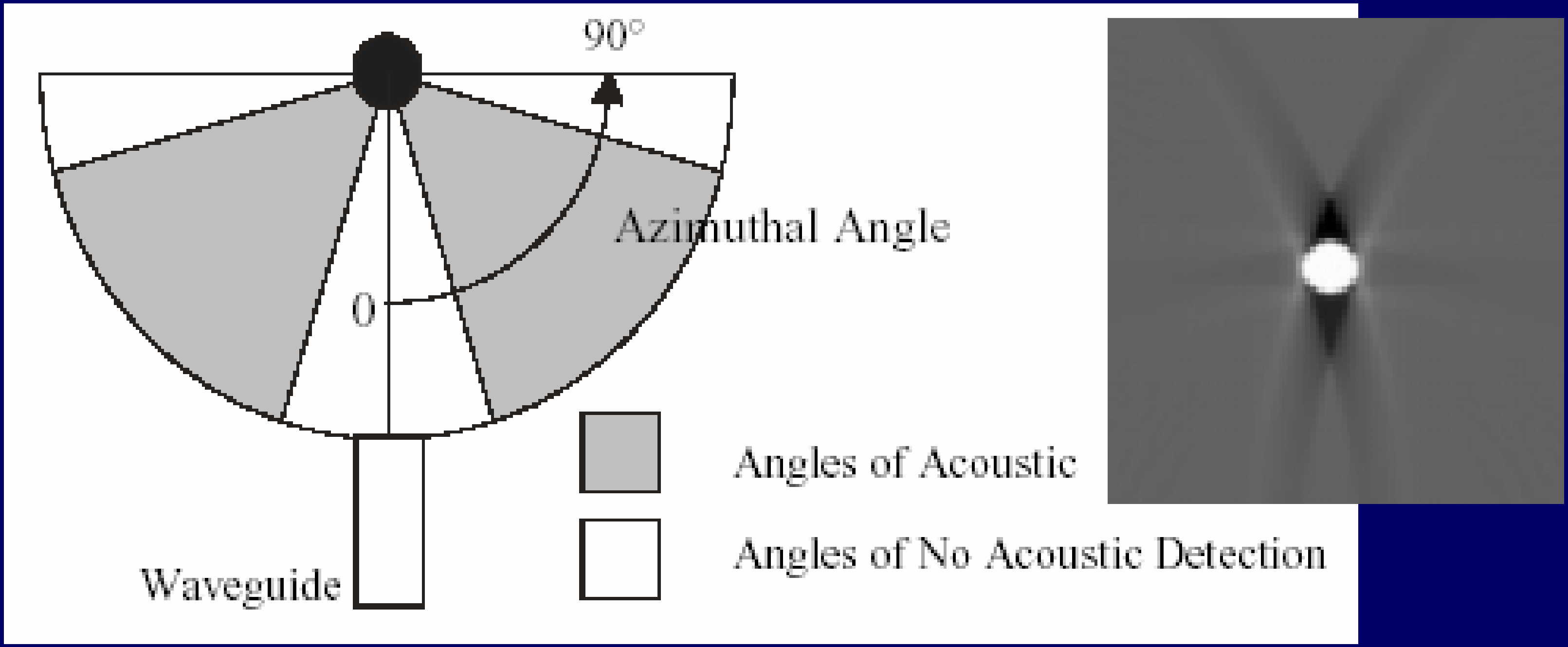

Images of a Human Breast

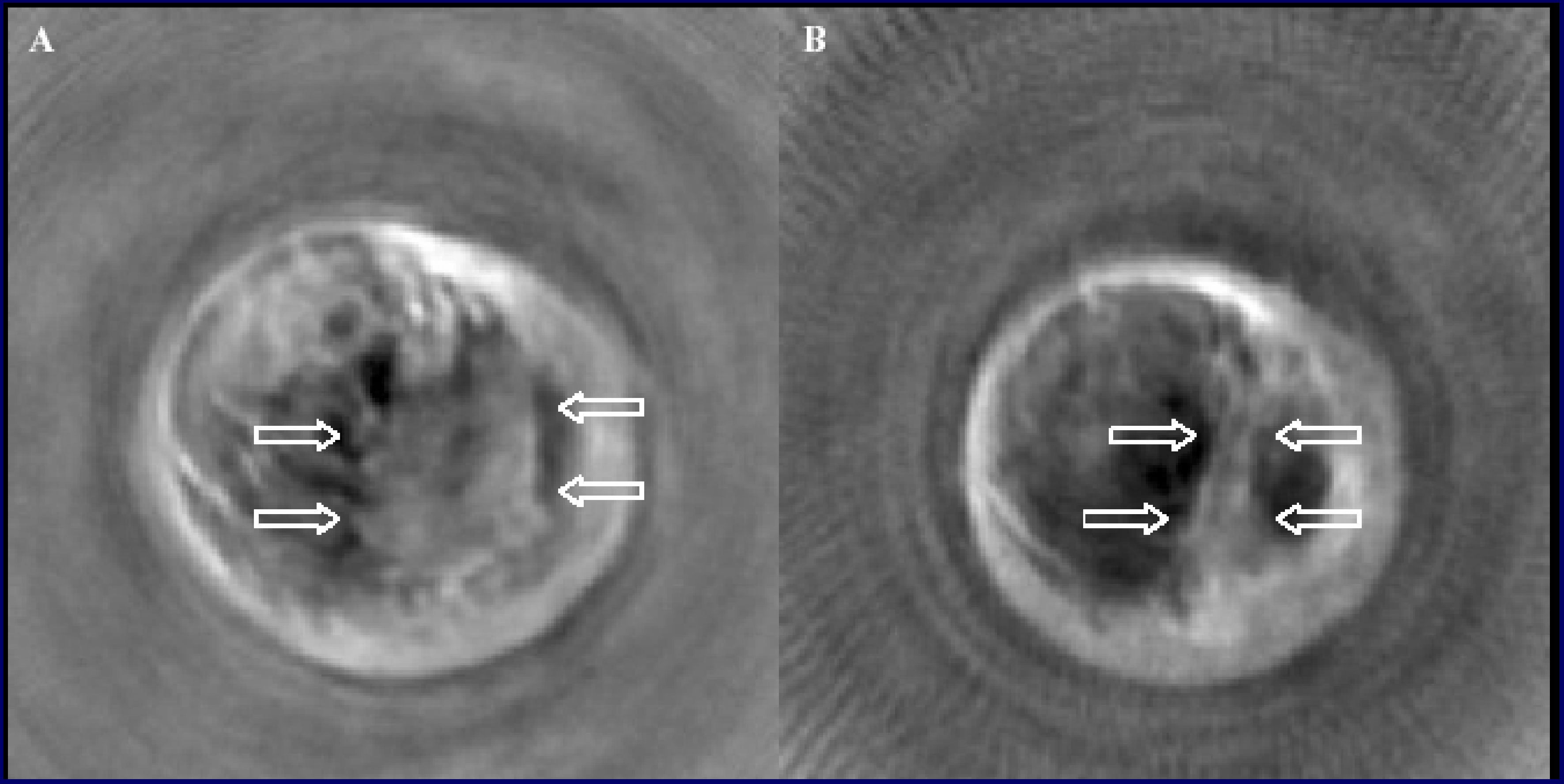

Cancerous Mass (before) Cancerous Mass (after)

Other Imaging Geometries

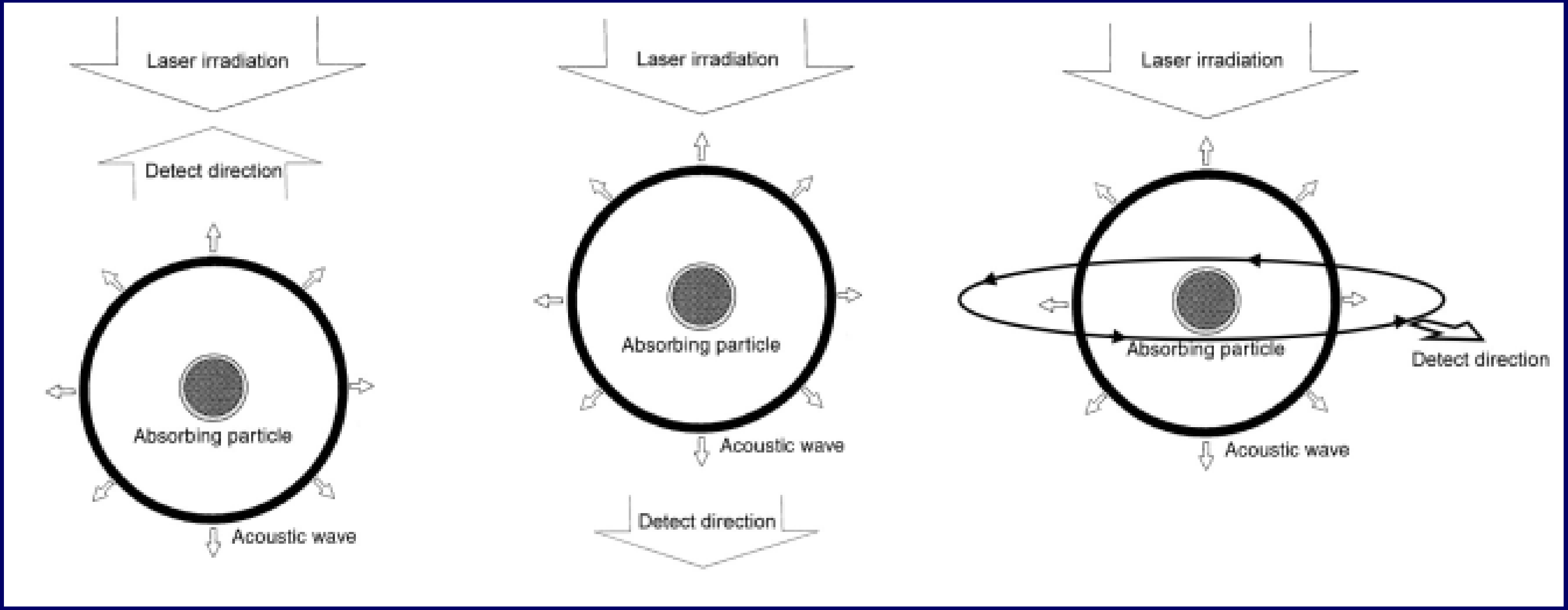

Depth Profiling of Absorbing Soft Materials Using Photoacoustic Methods [24]

OAT Depicts Tissue Layered Structure

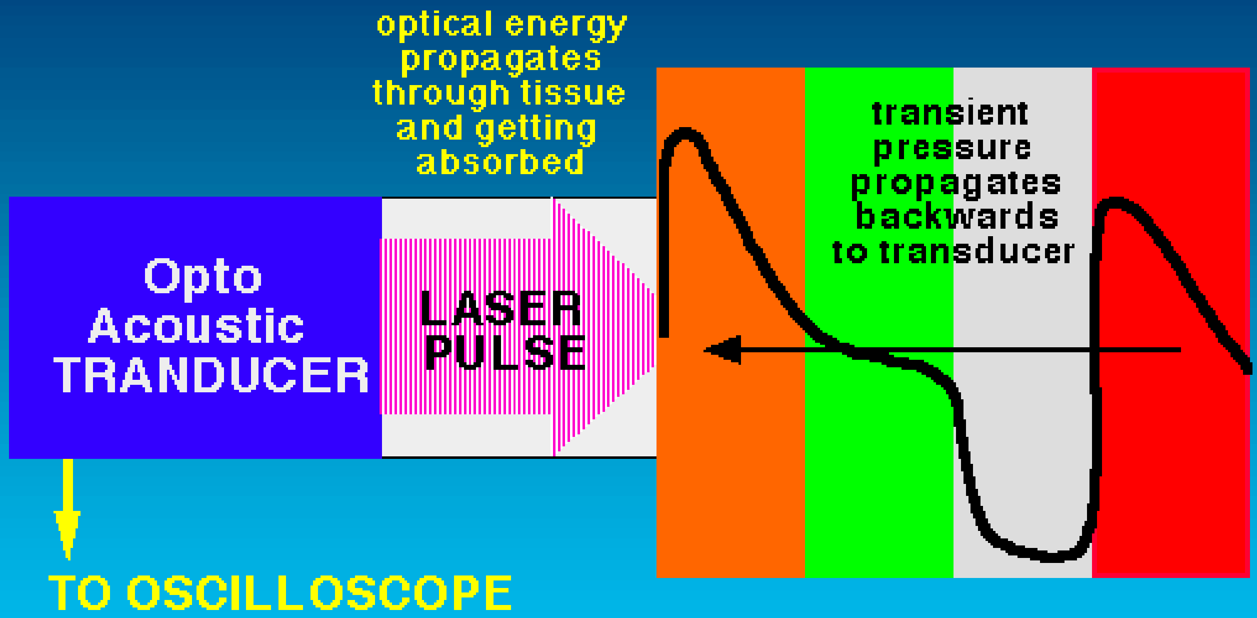

Direct visualization of layered tissue structure

$\Delta Z \approx \Delta t\ C_s = 8\ \text{ns} \cdot 1.5\ \mu\text{m/ns} = 12\ \mu\text{m}$

Confocal Opto-Acoustic Transducer

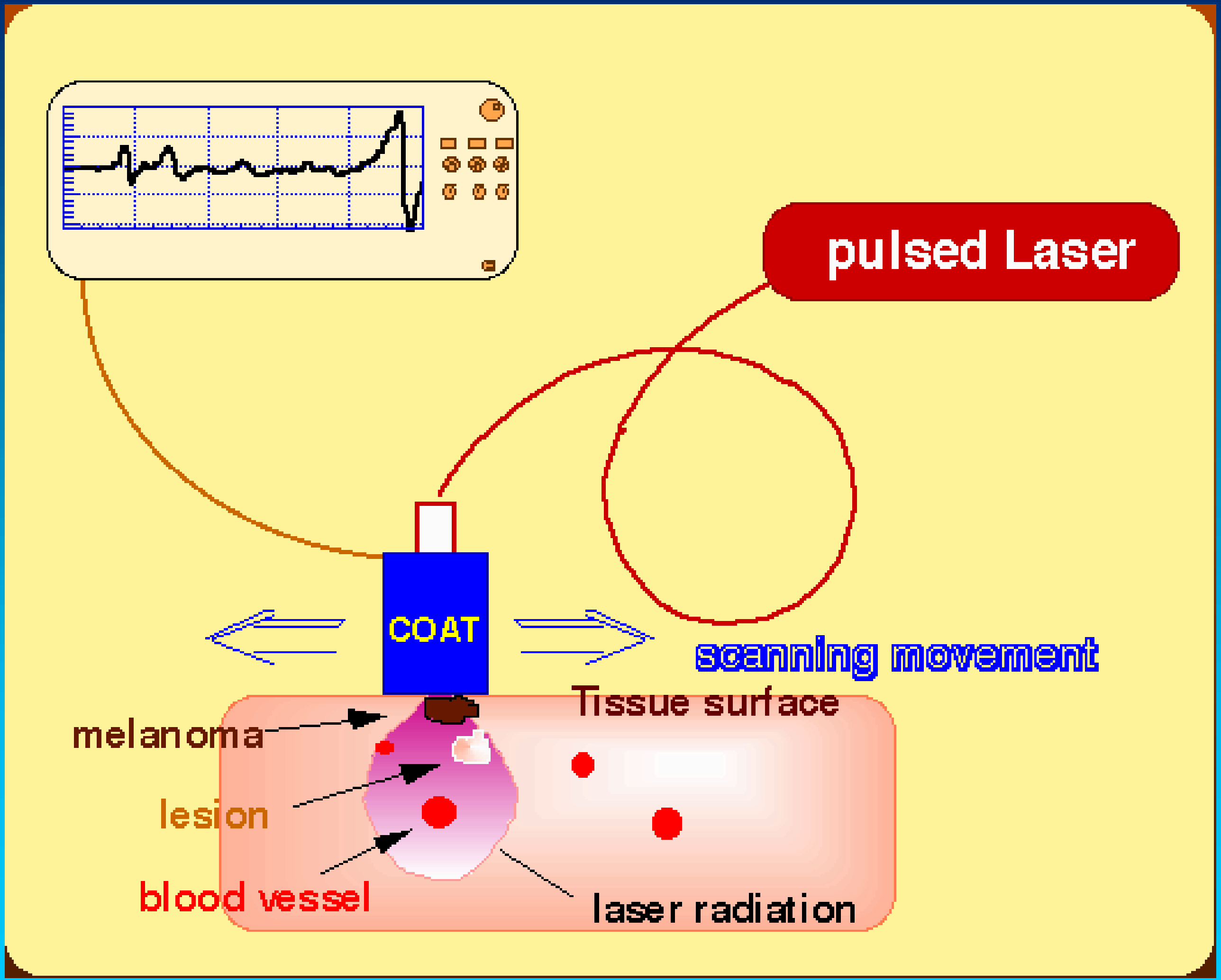

Schematic Diagram of COAT

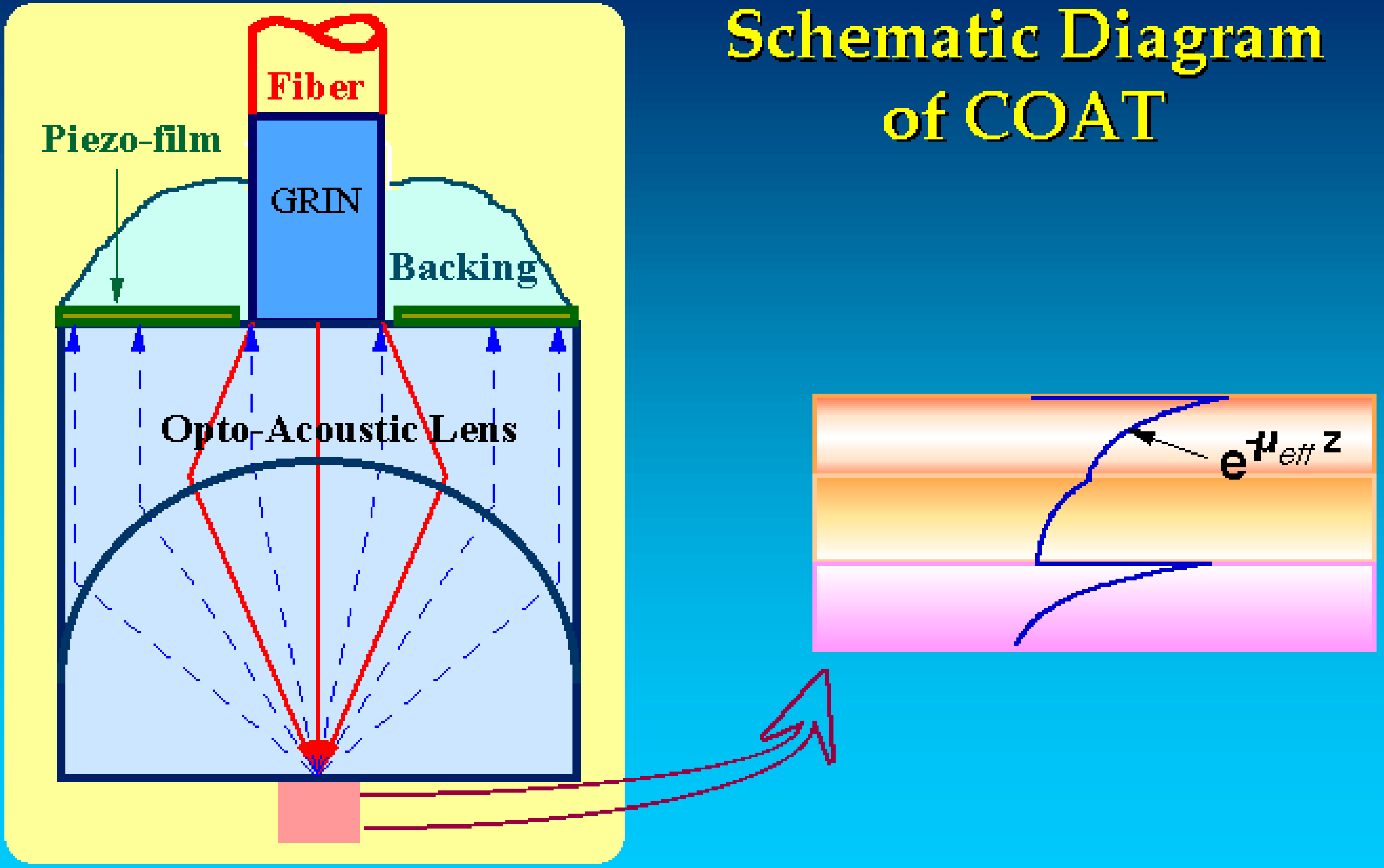

Confocal Opto-Acoustic Transducer

- Bandwidth 1÷100 MHz
- Resolution: 15 μm / 80 μm
- Sensitivity: 2 μV/Pa
- Depth of imaging: 2 mm

Laser pulse energy used: 10-100 μJ
Wavelength: 760 nm - 355 nm
Pulse duration: 10 ns

In vivo Opto-Acoustic Imaging of Oral Cancer in Syrian Golden Hamsters

Optoacoustic image and histology of normal pouch

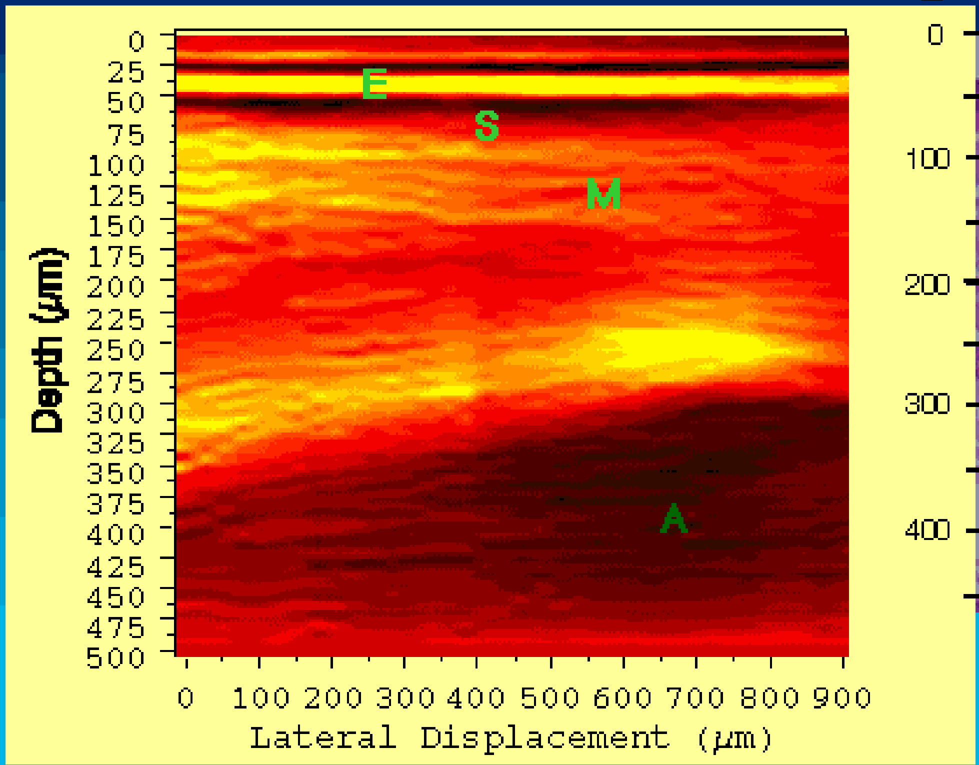

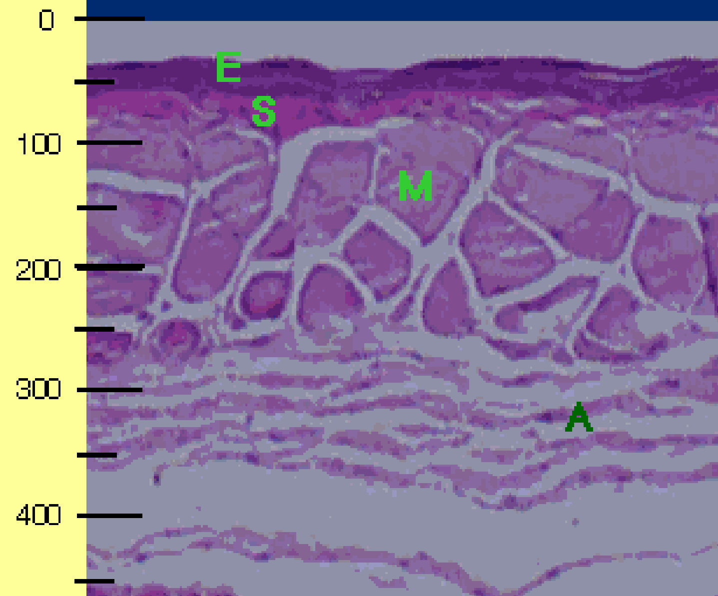

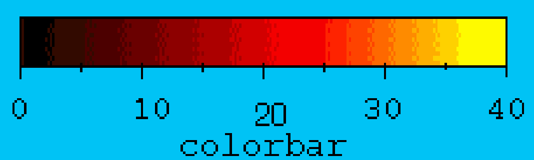

E-epithelium

S- submucosal connective tissue

M- striated muscle fiber mucosa

A- loose areolaconnective tissue

Optoacoustic image and H&E histology of very early cancer

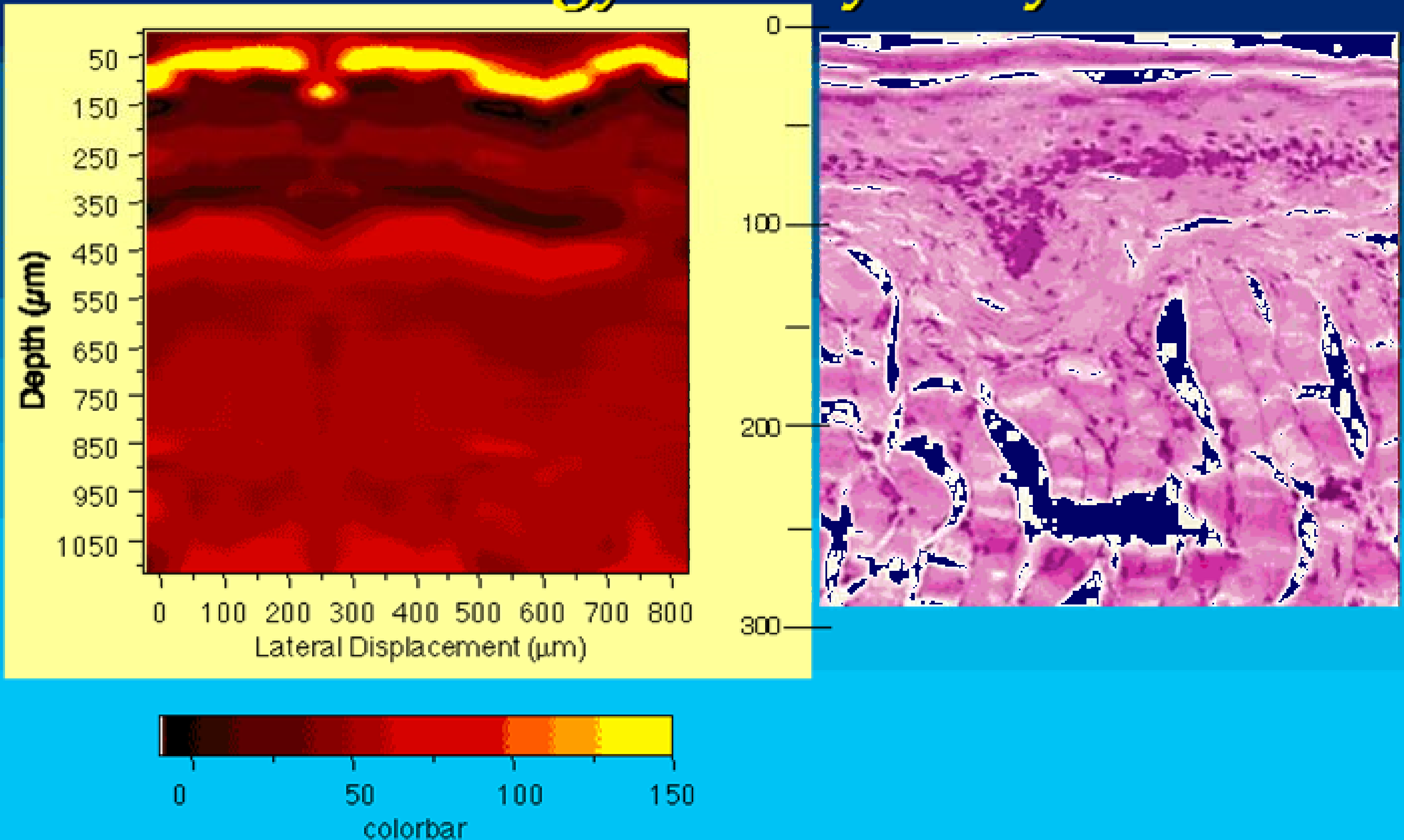

Optoacoustic image and H&E histology of carcinoma *in situ*.

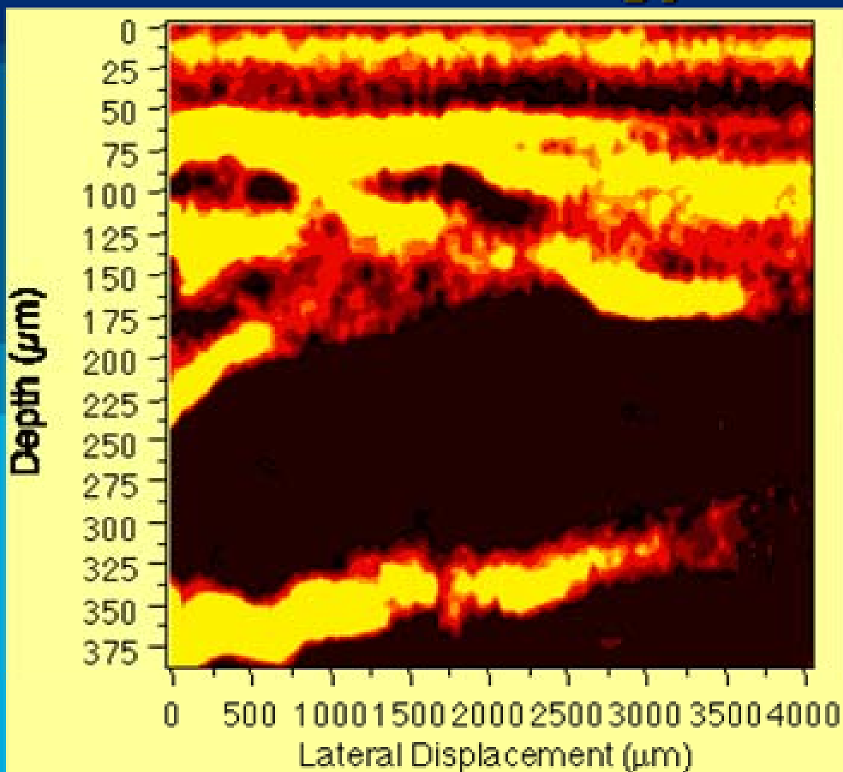

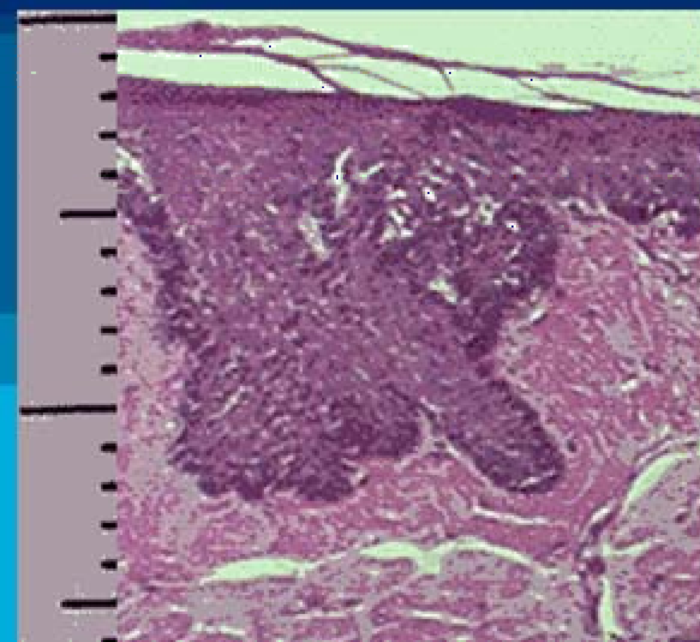

Optoacoustic image and histology of advanced stage of cancer

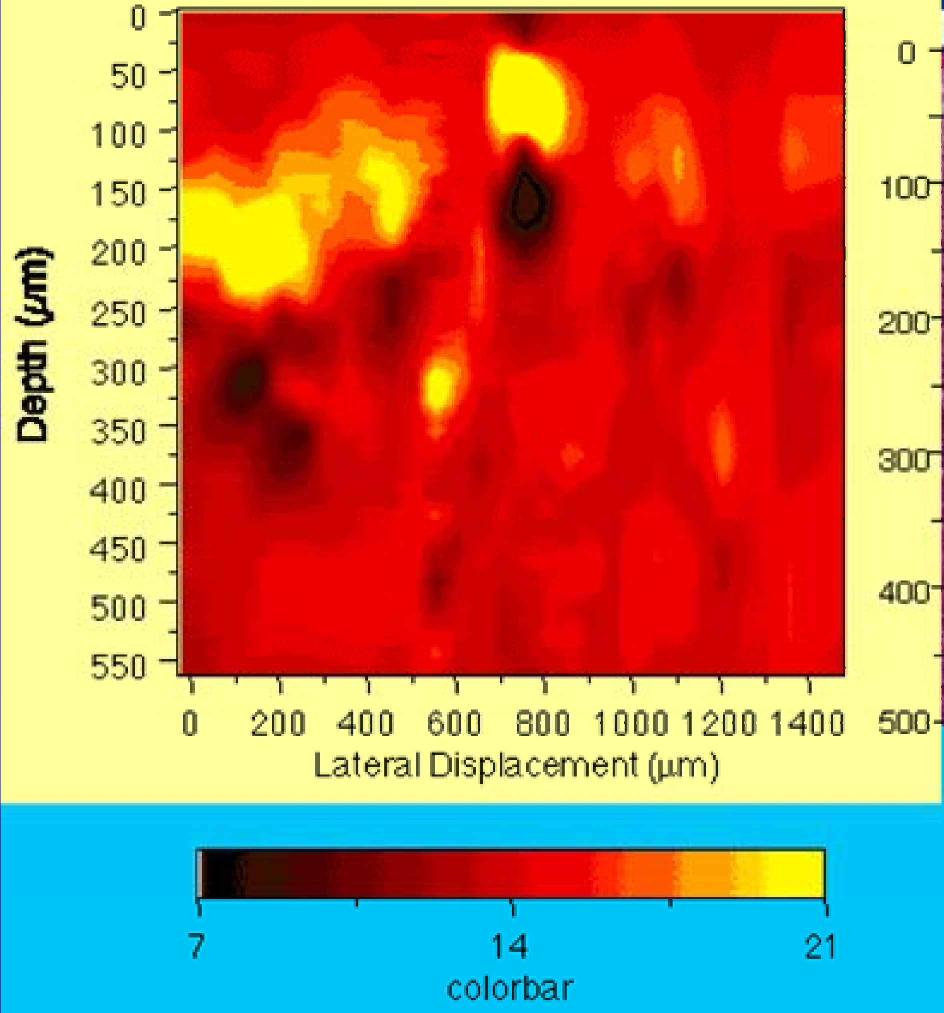

Sensitivity of Laser Opto-Acoustic Imaging in Detection of Small Deeply Embedded Tumors [4]

Motivation

- Develop an imaging technique for low contrast, small tumors.
- Optical contrast mechanism (between normal tissue and tumor):
  - Absorption: blood content, porphyrins.
  - Scattering: micro-structures.

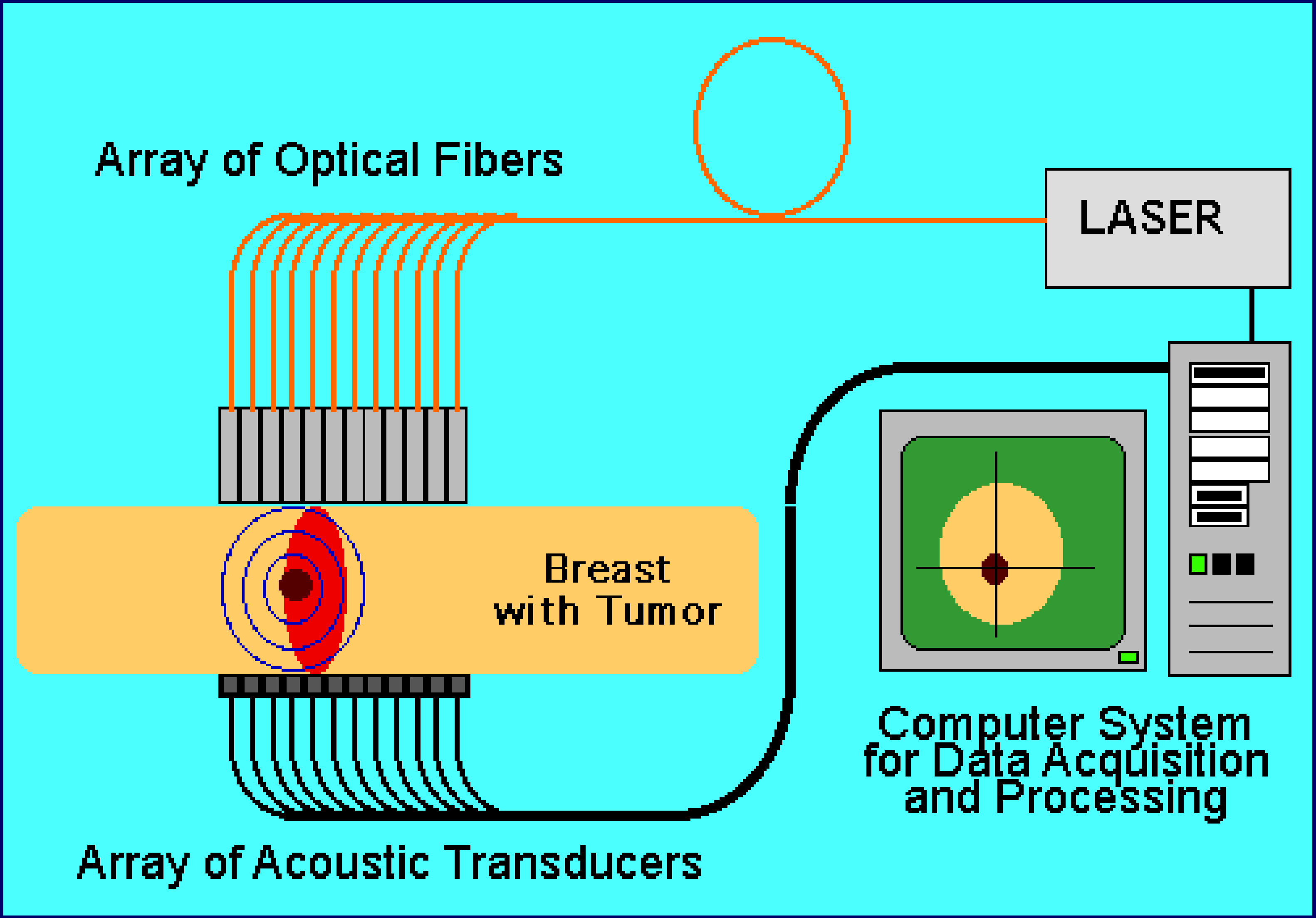
Array of Optical Fibers
LASER
Breast
with Tumor
Computer System
for Data Acquisition
and Processing
Array of Acoustic Transducers

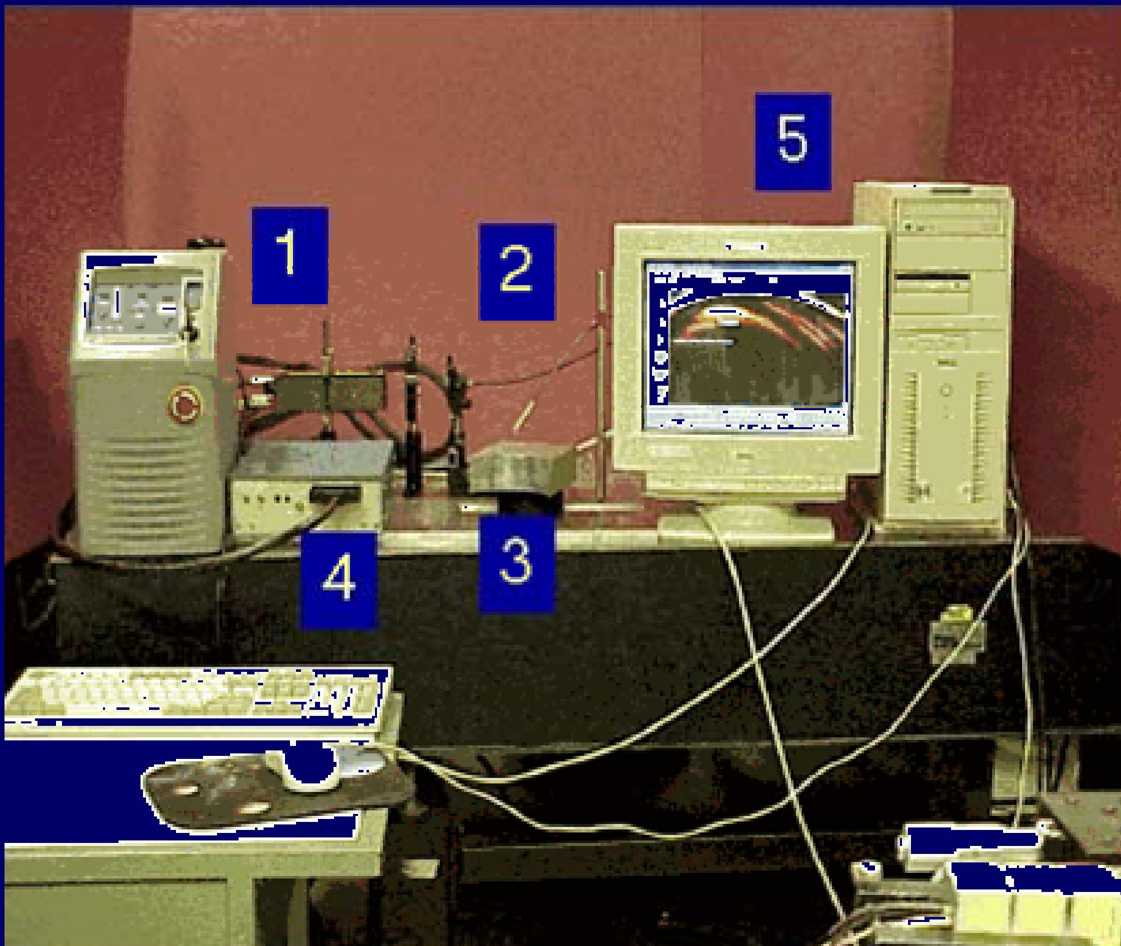

1 - Nd:YAG Laser
2 - Optical Fiber
3 - Arc Array of 32 transducers
4 - Amplifier and Multiplexor
5 - Computer

• Transducer Array:	32 of 1mm
• Sensitivity:	10 μV/Pa
• Resolution:	0.4 mm x 1 mm
• Data acquisition :	16 sec
• Data processing and image formation:	4 sec
• Image processing:	15 sec
• Total time:	35 sec

Sensitivity of Tumor Detection

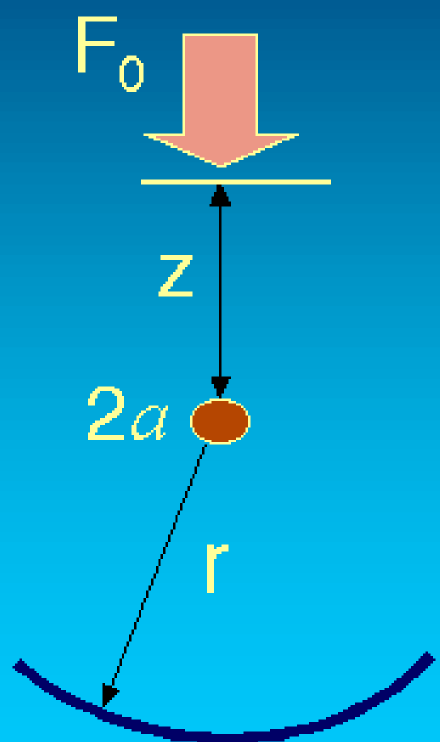

$$z_{\max} = -\frac{1}{\mu_{eff}} \ln\left(\frac{2 p_N r}{\Gamma \mu_a a F_0}\right)$$

p_N - Noise pressure (SNR =1)

Maximum Depth of Tumor Detection

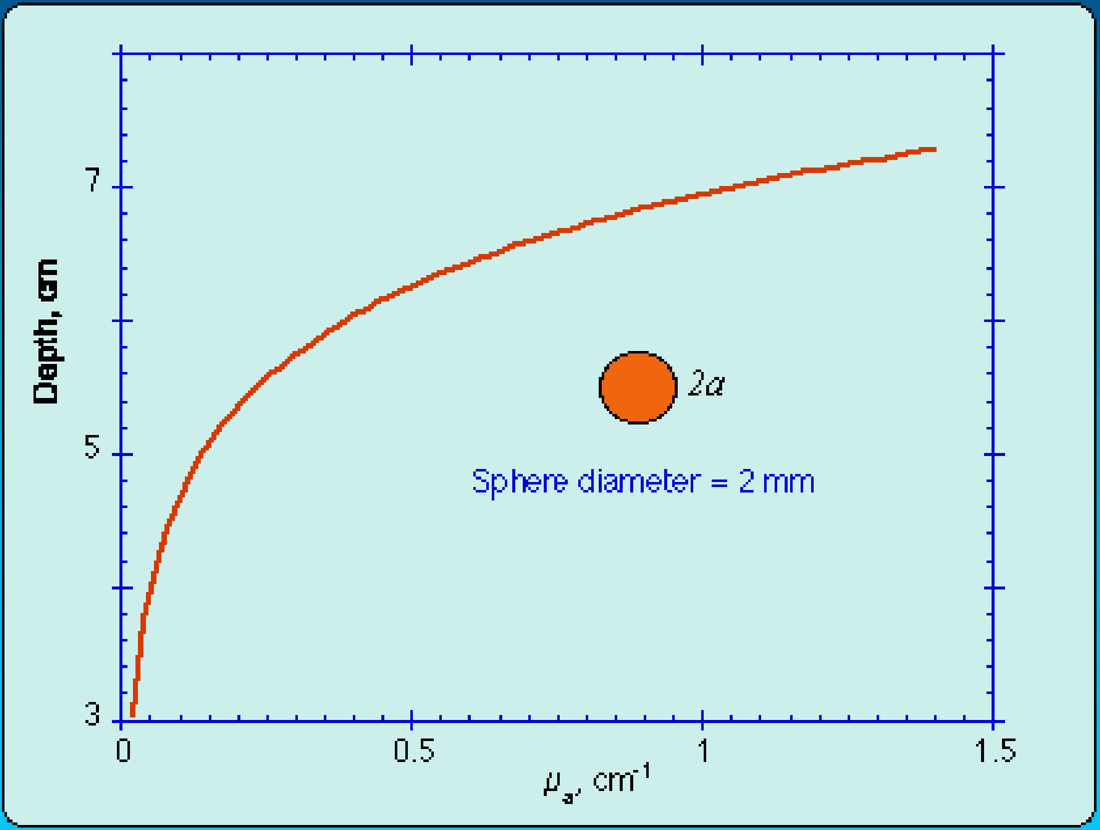

Signal Processing Diagram

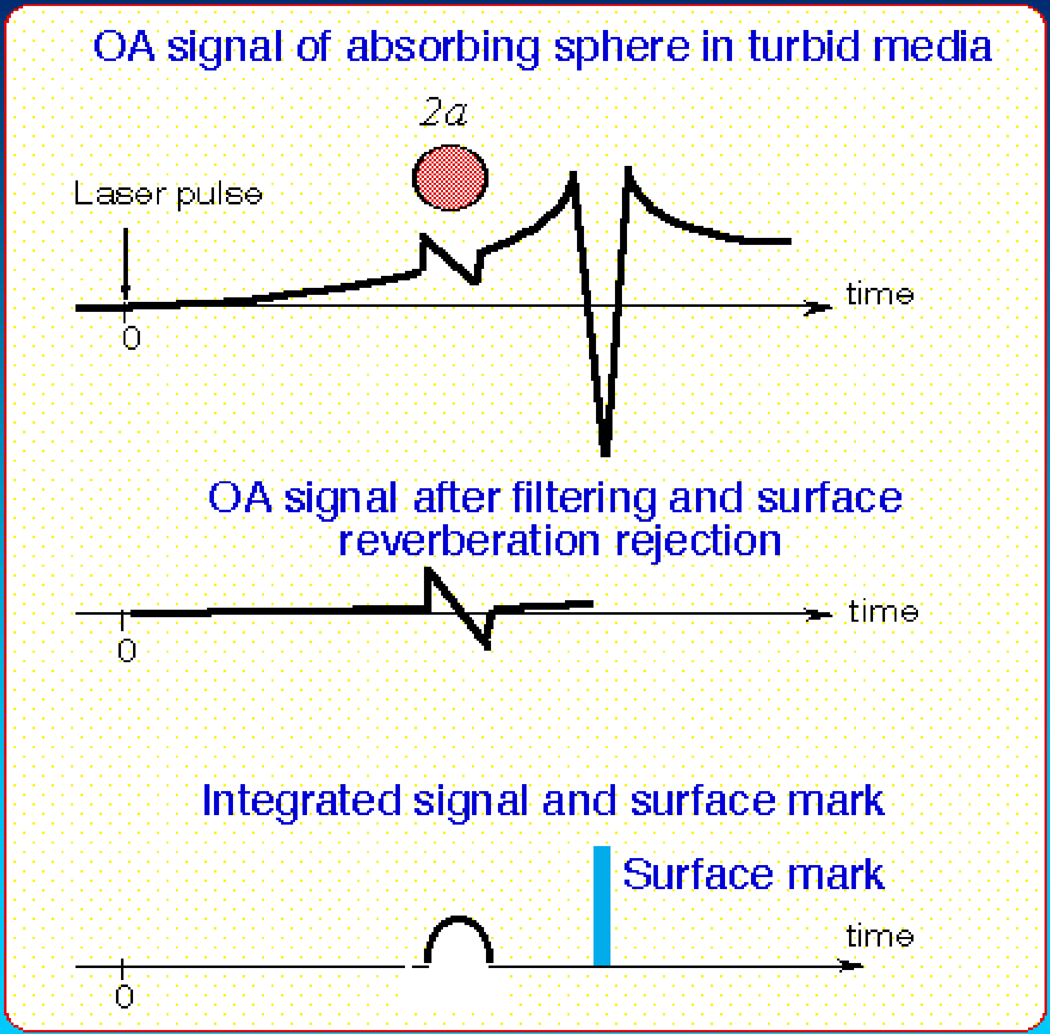

N - Shaped Optoacoustic Signals from Small Spheres

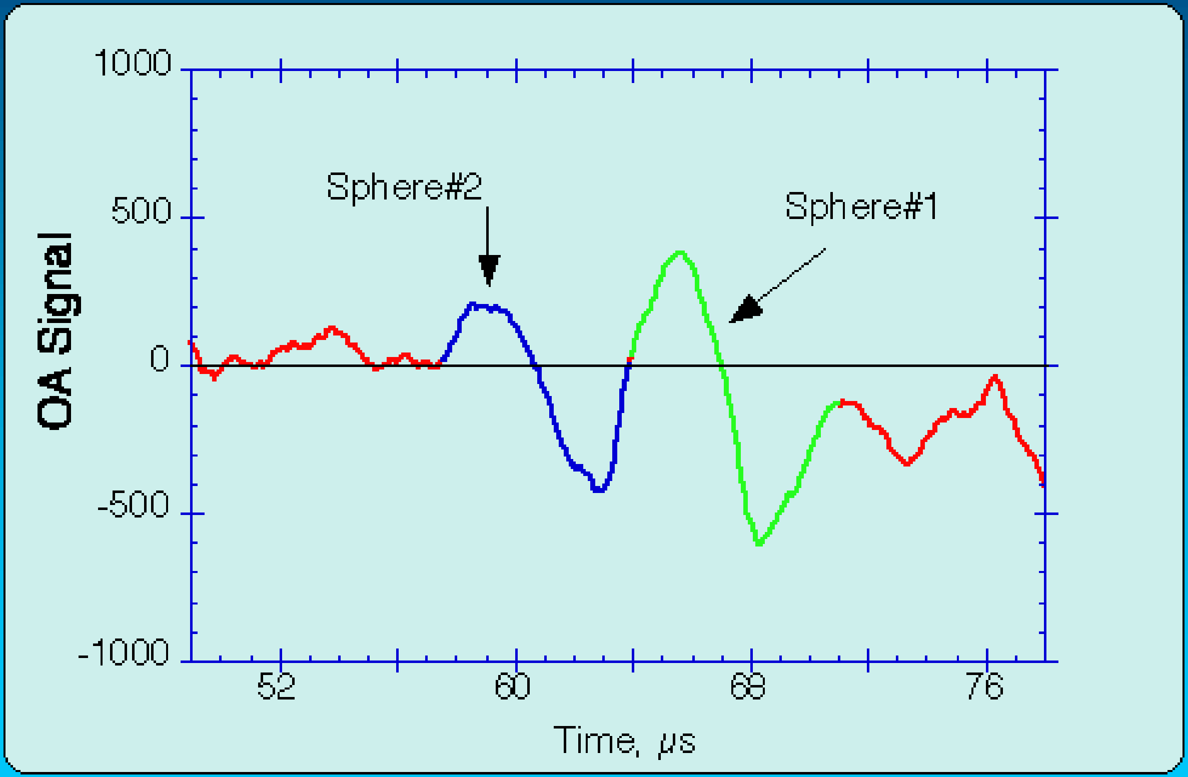

Optoacoustic Imaging Equation

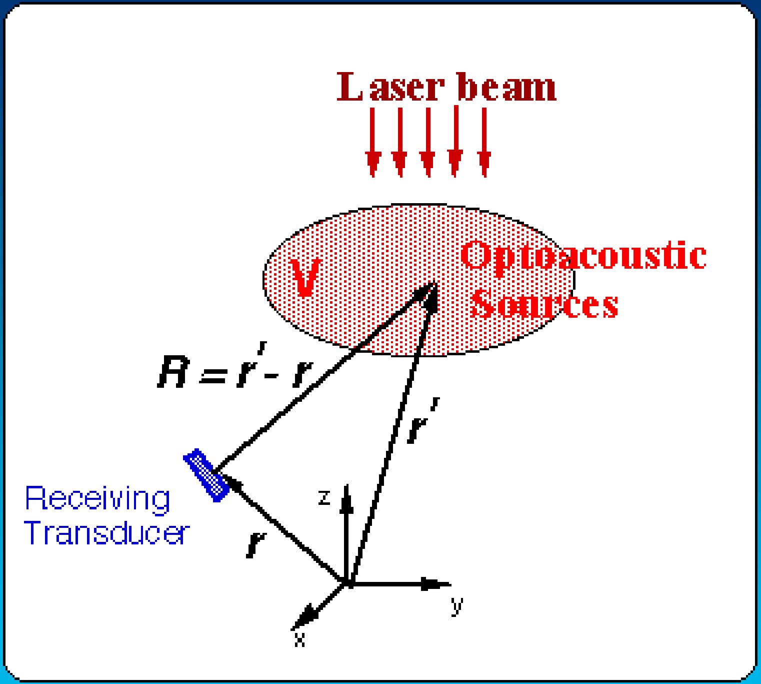

$$u(r,t) = \int_{-\infty}^{t} p'(\vec{r},\tau)d\tau = \frac{\beta}{4\pi C_p}\int_V \frac{\mu_a(\vec{r}')I(\vec{r}')L(t - \frac{|\vec{r}-\vec{r}'|}{c_s})}{|\vec{r}-\vec{r}'|}dr'$$

Image Reconstruction Algorithm

- Radial Backprojection

$$\xi(\vec{r}) = \sum_{n=1}^{N} u_n\left(\left|\vec{r} - \vec{r}_n\right| / c_s\right)\left|\vec{r} - \vec{r}_n\right|$$

Image Processing

Filtration of the entire image matrix, $\xi_2(\vec{r})$

$$\xi_2(\vec{r}) = \frac{1}{4\pi^2} \int F_\xi(\vec{\omega}) H(\vec{\omega}) e^{i\vec{\omega}\vec{r}} d\vec{\omega}$$

$F_\xi(\vec{\omega}) = \int \xi(\vec{r}) e^{-i\vec{\omega}\vec{r}} d\vec{r}$ – *Spatial FFT Spectrum*

$H(\vec{\omega}) = |\vec{\omega}| e^{-(|\vec{\omega}|/\sigma)^2}$ – *Filter Transfer Function*

Gelatin Phantom

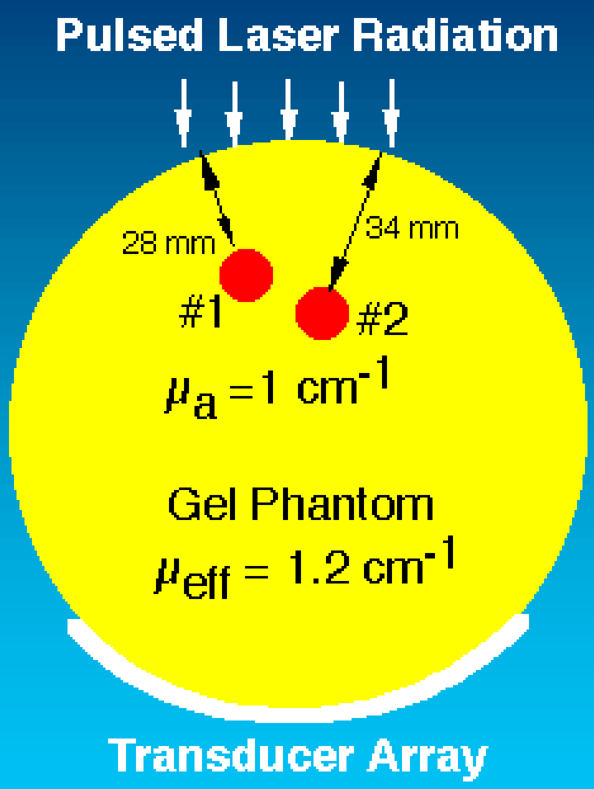

- 2 spheres were embedded in phantom of 120-mm diameter.
- Light absorption coefficient of spheres : $\mu_a = 1.0\ cm^{-1}$.
- Light attenuation coefficient of phantom: $\mu_{eff} = 1.2\ cm^{-1}$.

OA Image of Two Spheres in Gel Phantom

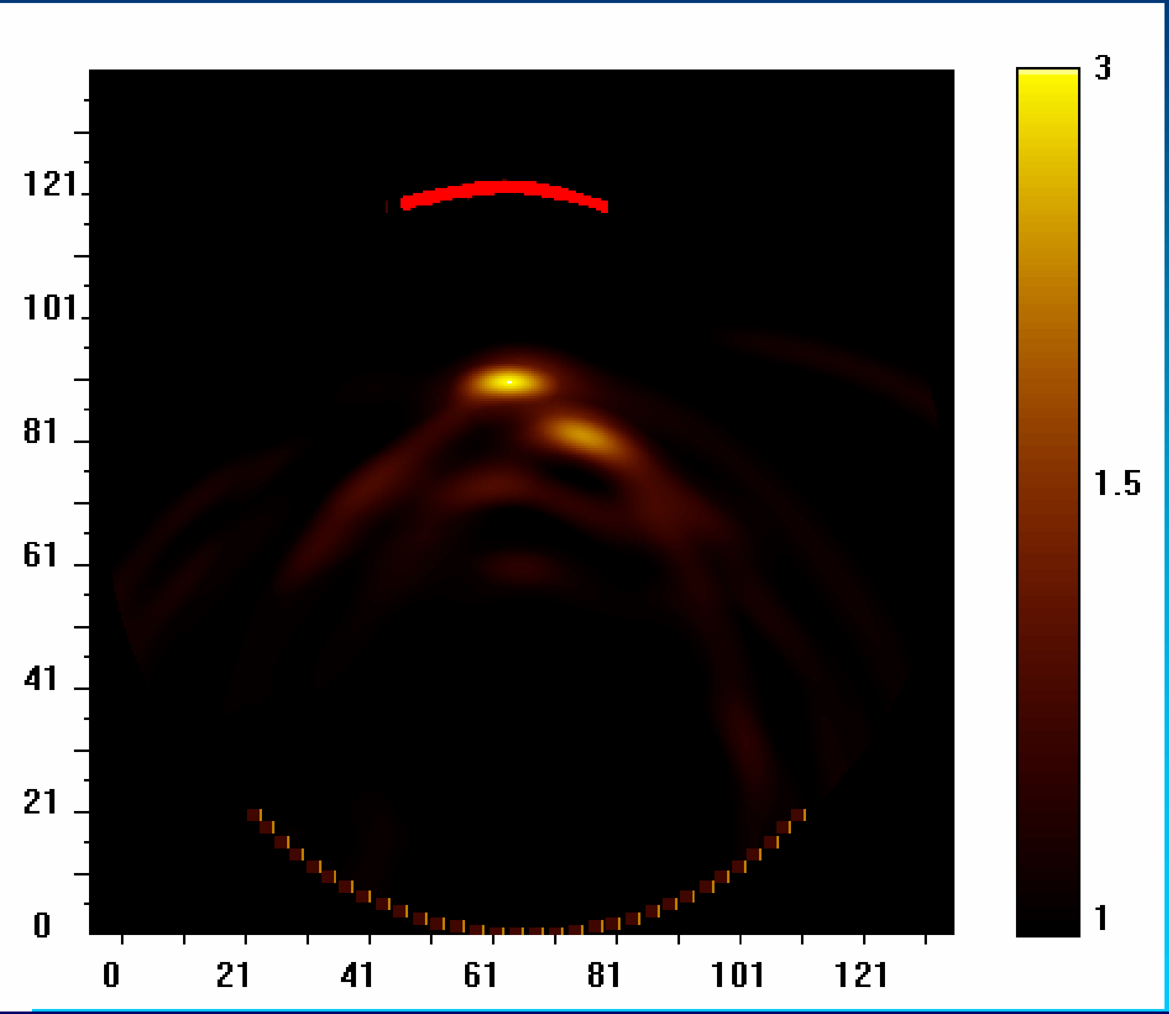

Is Functional Opto-acoustic Imaging Possible?

Structural and Functional Mouse Brain OA Imaging [18]

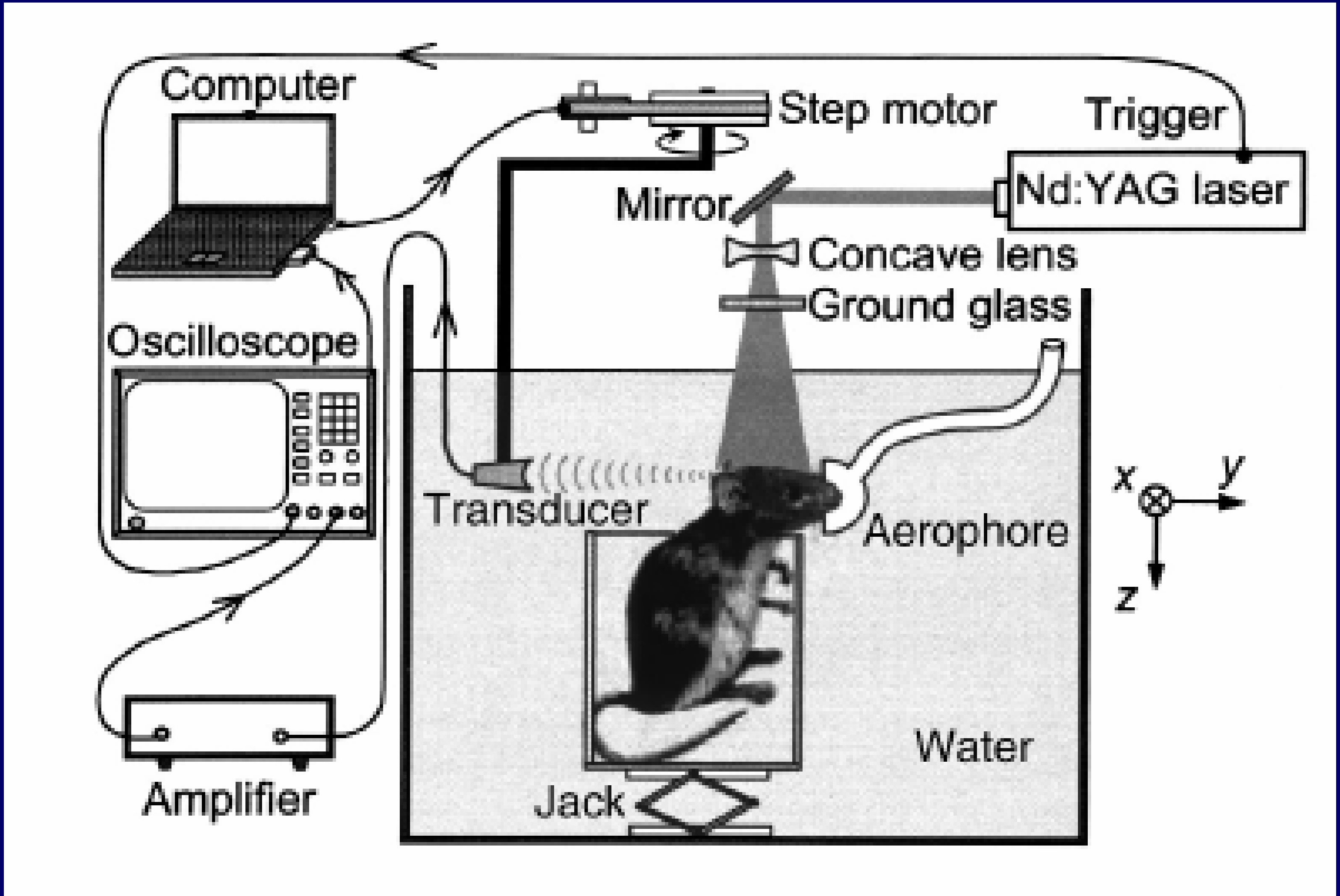

Mouse Brain Structural Image

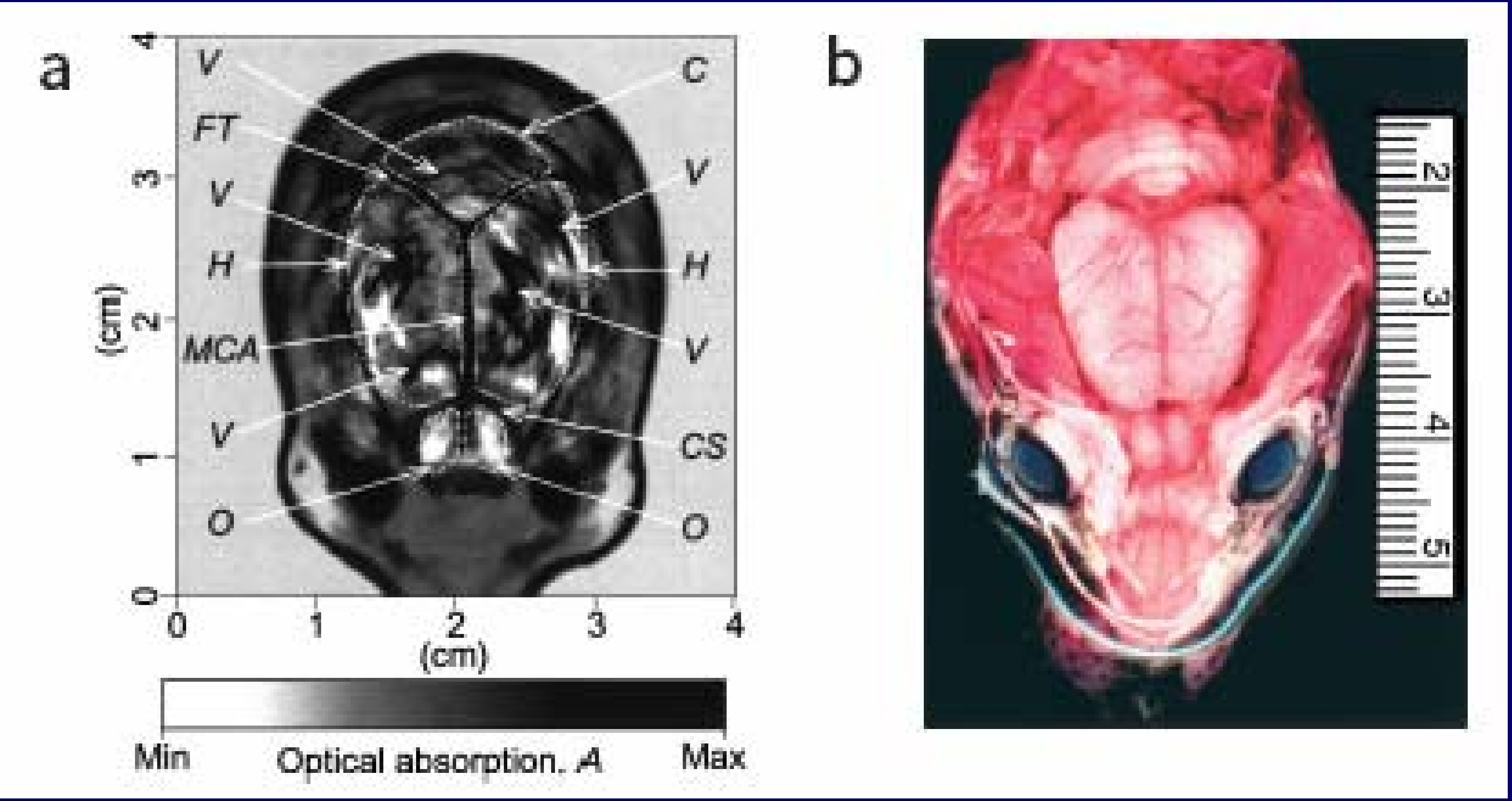

Mouse Brain Functional Image

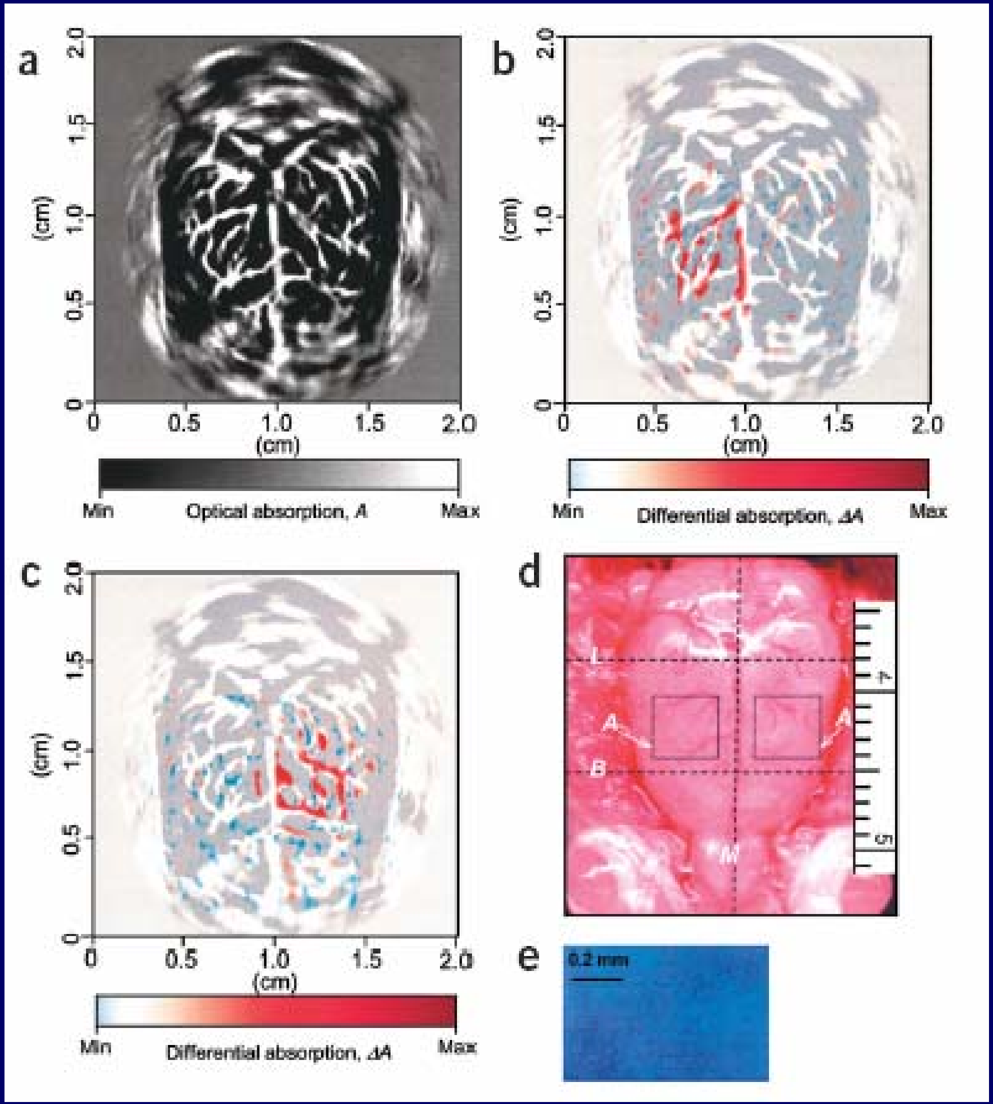

Blood Oxygenation Detection

Dual Wavelength Technique

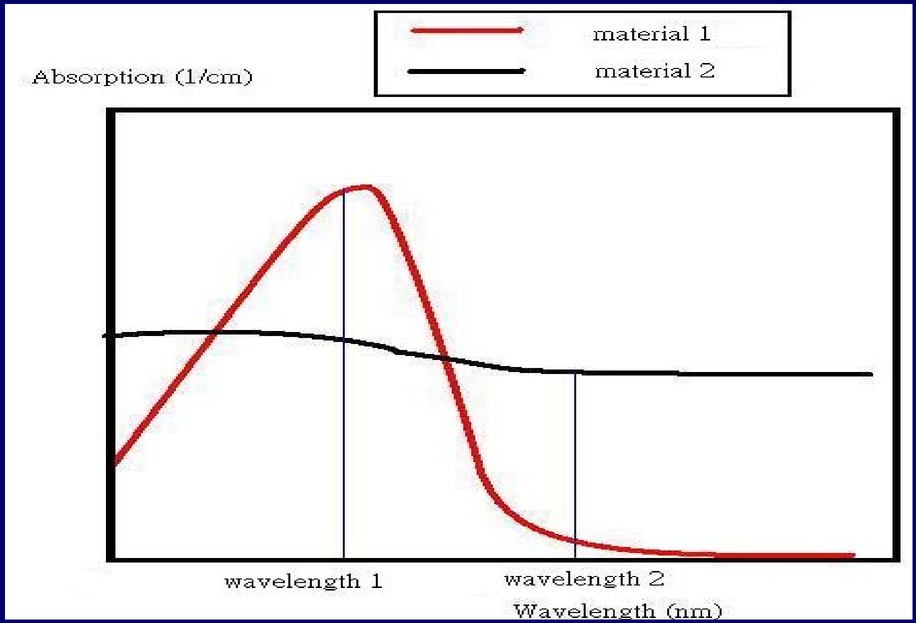

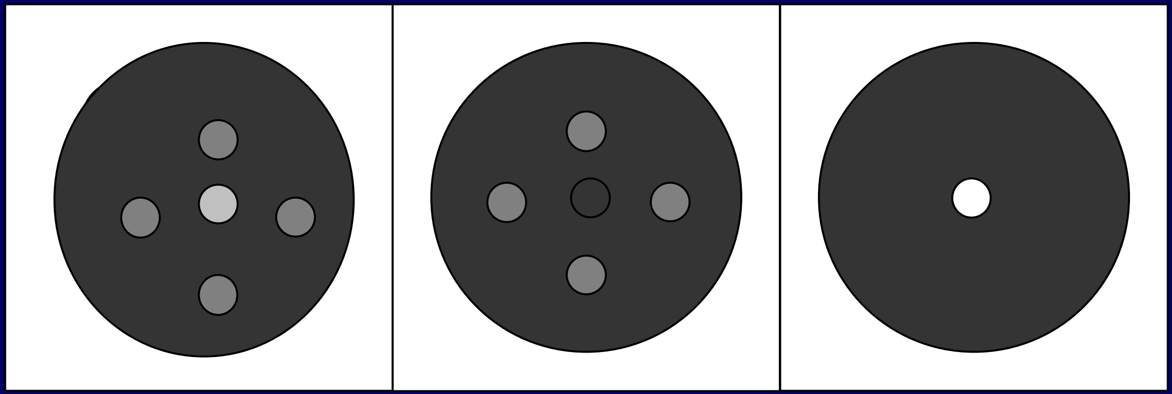

Blood Oxygenation Detection

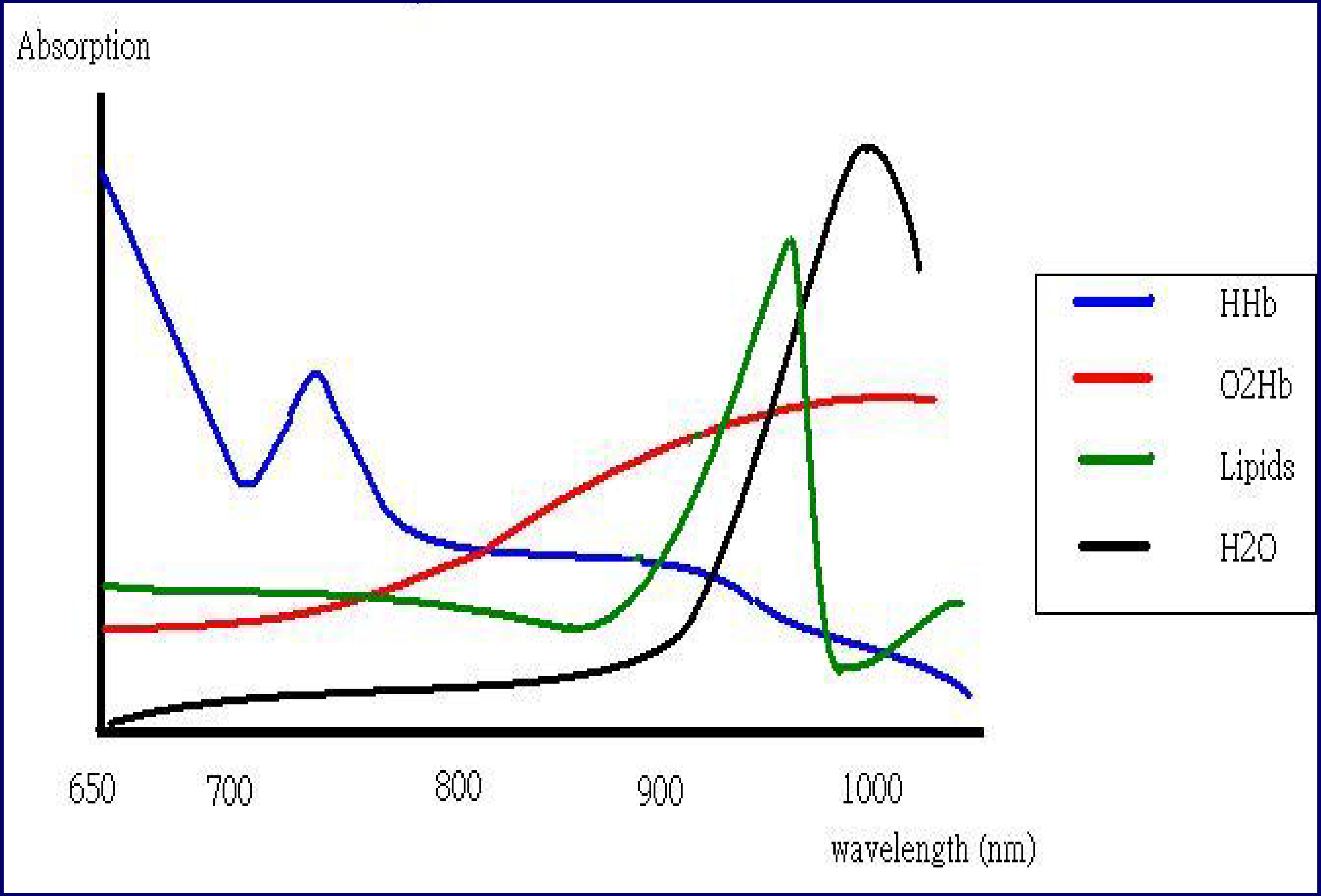

Opto-acoustic Molecular Imaging

Gold Nanoparticles

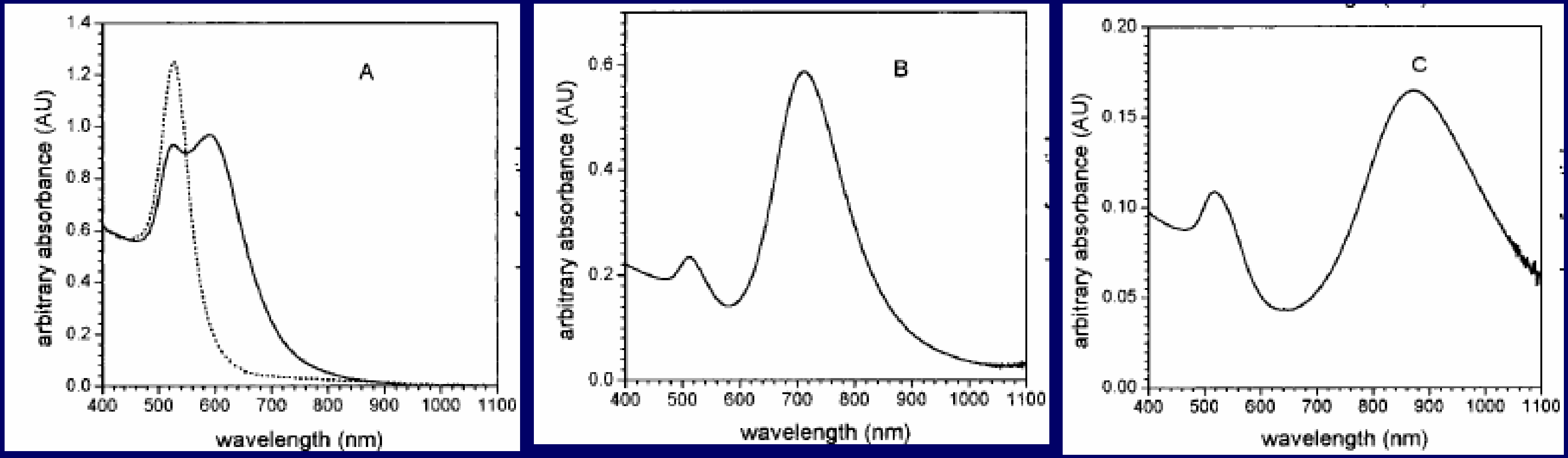

Gold Nanoparticles

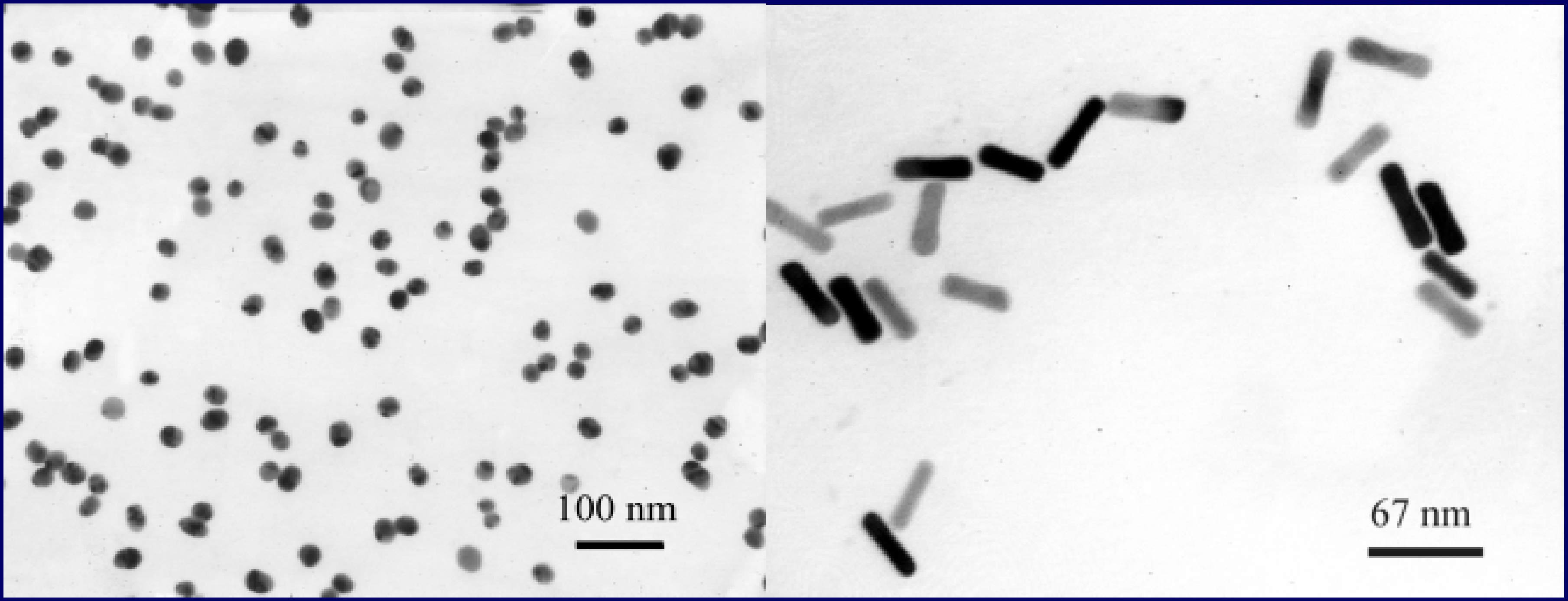

References

References

1. A. A. Karabutov and V. E. Gusev, Laser optoacoustics (American Institute of Physics, New York, 1993).
2. A. A. Karabutov, E. V. Savateeva, N. B. Podymova, and A. A. Oraevsky, “Backward mode detection of laser-induced wide-band ultrasonic transients with optoacoustic transducer,” J. Appl. Phys. vol. 87, no. 4, pp.2003–2014 (2000).
3. A. A. Karabutov, N. B. Podymova, and V. S. Letokhov, “Time-resolved laser optoacoustic tomography of inhomogeneous media,” Appl. Phys. vol.63, pp.545–563 (1996).
4. R. O. Esenaliev, A. A. Karabutov, and A. A. Oraevsky, “Sensitivity of laser opto-acoustic imaging in detection of small deeply embedded tumors,” IEEE J. Sel. Top. Quantum Electron. vol. 5, pp.981–988 (1999).
5. J. A. Viator, L. O. Svaasand, G. Aguilar, B. Choi, and J. S. Nelson, “Photoacoustic measurement of epidermal melanin,” in Biomedical optoacoustics IV, A. A. Oraevsky, ed. Proc. SPIE 4960, pp.14–20 (2003).
6. C. G. A. Hoelen, F. F. M. de Mul, R. Pongers, and A. Dekker, “Three-dimensional photoacoustic imaging of blood vessels in tissue,” Opt. Lett. vol. 23, no. 8, pp.648–650 (1998).

References (Cont.)

7. R. O. Esenaliev, I. V. Larina, K. V. Larin, D. J. Deyo, M. Motamedi, and D. S. Prough, “Optoacoustic technique for noninvasive monitoring of blood oxygenation: a feasibility study,” Appl. Opt. vol. 41, no.22, pp.4722–4731 (2002).
8. A. A. Oraevsky, S. L. Jacques, and F. K. Tittel, “Measurement of tissue optical properties by time-resolved detection of laser-induced transient stress,” Appl. Opt. vol. 36, no. 1 pp.403-415 (1997).
9. Y. Xu, D. Feng, and L. V. Wang, ”Exact frequency-domain reconstruction for thermoacoustic tomography-I: planar geometry,” IEEE trans. Medical imaging, vol. 21, no. 7, pp.823-828 (2002).
10. Y. Xu, D. Feng, and L. V. Wang, ”Exact frequency-domain reconstruction for thermoacoustic tomography-II: cylindrical geometry,” IEEE trans. Medical imaging, vol. 21, no. 7, pp.829-833 (2002).
11. R. A. Kruger, W. L. Kiser Jr, D. R. Reinecke, G. A. Kruger, and K. D. Miller,” Thermoacoustic optical molecular imaging of small animals,” Molecular Imaging vol. 2, no. 2, pp.113-123 (2003).
12. R. A. Kruger, W. L. Kiser Jr, D. R. Reinecke, and G. A. Kruger, “Thermoacoustic computed tomography using a conventional linear transducer array,” Medical Physics vol. 30, no. 5, pp.856-860 (2003).

References (Cont.)

13. R. A. Kruger, K. M. Stantz, and W. L. Kiser Jr, “Thermoacoustic CT of the Breast,” Proc. SPIE vol. 4682, pp.521-525 (2002).
14. R. A. Kruger and W. L. Kiser Jr, ”Thermoacoustic CT of the Breast: Pilot Study Observations,” Proc. SPIE vol. 4256, pp.1-5 (2001).
15. R. A. Kruger, W. L. Kiser Jr, K. D. Miller, and H. E. Reynolds, “Thermoacoustic CT: imaging principles,” Proc SPIE vol. 3916, pp.150-159 (2000).
16. R. A. Kruger, “Photoacoustic ultrasound,” Med. Phys. vol. 21, no. 1, pp.127-131 (1994)..
17. R. A. Kruger, R. Liu, Y. Fang, and C. R. Appledom, ”Photoacoustic ultrasound (PAUS)-reconstruction tomography,” Med. Phy. vol. 22, no. 10, pp. 1605-1609 (1995).
18. X. Wang, Y. Pang, G. Ku, X. Xie, G. Stoica, and L. V. Wang, “Noninvasive laser-induced photoacoustic tomography for structural and functional in vivo imaging of the brain,” Nature Biotech. vol. 21, no. 7, pp.803-806 (2003).

References (Cont.)

19. X. Wang, Y. Pang, G. Ku, G. Stoica, and L. V. Wang, "Three-dimensional laser-induced photoacoustic tomography of mouse brain with the skin and skull intact," Optics Lett. vol. 28, no. 19, pp.1739-1741 (2003).
20. M. Xu, Y. Xu, and L. V. Wang, "Time-domain reconstruction algorithms and numerical simulations for thermoacoustic tomography in various geometries," IEEE Tran. Biomedical engineering. vol. 50, no. 9, pp. 1086-1099 (2003).
21. M. Xu and L. V. Wang, "Time-domain reconstruction for thermoacoustic tomography in a spherical geometry," IEEE Tran. Medical Imaging, vol. 21, no. 7, pp. 814-822 (2002).
22. Xu and L.V. Wang, "Effects of acoustic heterogeneity in breast thermoacoustic tomography," IEEE Trans. Ultrason., Ferroelect., Freq. Contr., vol. 50 no. 9, pp. 1134-1146 (2003).
23. A. A. Oraevsky, A. N. Oraevsky, " Plasmon resonance in ellipsoid nanoparticles," Quant. Electron. vol. 32, no. 1, pp.79-82 (2002).

References (Cont.)

24. J. A. Viator, S. L. Jacques and S. A. Prahl, “Depth profiling of absorbing soft materials using photoacoustic methods”, IEEE Journal of Selected Topics in Quantum Electronics, vol. 5, no. 4, pp 989-996 (1999).
25. J. D. Hamilton, T. Buma, M. Spisar, M. O’Donnell, ”High frequency optoacoustic arrays using etalon detection,” IEEE Trans. Ultrason. Ferroelectr. Freq. Control, vol. 47, no. 1, pp160-168 (2000).
26. J. D. Hamilton, C. J. Brooks, G. L. Vossler, M. O’Donnell, ”High frequency ultrasound imaging using a active optical detector,” IEEE Trans. Ultrason. Ferroelectr. Freq. Control, vol. 45, no. 3, pp719-727 (1998).